

INVESTIGATING THE RELATIONSHIP BETWEEN
CARDIAC FUNCTION AND INSULIN SENSITIVITY
IN HORSES

By

NATASHA WILLIAMS

Bachelor of Science in Molecular and Drug Design
University of Adelaide
Adelaide, South Australia, Australia
2008

Bachelor of Veterinary Science
University of Melbourne
Melbourne, Victoria, Australia
2013

Submitted to the Faculty of the
Graduate College of the
Oklahoma State University
in partial fulfillment of
the requirements for
the Degree of
MASTER OF SCIENCE
December, 2021

INVESTIGATING THE RELATIONSHIP BETWEEN
CARDIAC FUNCTION AND INSULIN SENSITIVITY
IN HORSES

Thesis Approved:

Martin Furr

Thesis Adviser

Veronique Lacombe

Michael Davis

Robert Streeter

ACKNOWLEDGEMENTS

Drs Martin Furr, Veronique Lacombe, Cristobal Navas de Solis, Mike Davis, and Robert Streeter for their assistance in the study and much-valued mentoring.

Drs Allison Campolo, Benjamin Scherlag, Brianne Taylor, Erin McCarty, and Erik Clary, and Matthew Rochowski, Shawn Allen and Samantha Lazarowicz for their help in completion of various aspects of the study

FUNDING

Funding for this study was provided by awards from the Oklahoma State University College of Veterinary Medicine Research Advisory Committee, and the Oklahoma State University Vice President of Research.

Name: NATASHA WILLIAMS

Date of Degree: DECEMBER, 2021

Title of Study: INVESTIGATING THE RELATIONSHIP BETWEEN CARDIAC
FUNCTION AND INSULIN SENSITIVITY IN HORSES

Major Field: VETERINARY BIOMEDICAL SCIENCES

Abstract: Metabolic syndrome in humans is commonly associated with cardiovascular dysfunction, including atrial fibrillation and left ventricular diastolic dysfunction. Although many differences exist between human and equine metabolic syndrome, both of these conditions share some degree of insulin resistance. The aims of this study were to investigate the relationship between magnitude of insulin resistance and degree of myocardial dysfunction. Seven horses (five mares, two geldings, age 17.2 ± 4.2 years, weight 524 ± 73 kg) underwent insulin-modified frequently sampled intravenous glucose tolerance testing to determine insulin sensitivity (mean $2.21 \pm L/min/mU$). Standard echocardiograms were performed on each horse, including two-dimensional, M-mode, and pulse-wave tissue Doppler imaging. Data were assessed for normality by constructing normal probability plots and performing the Shapiro-Wilks test. Pearson and Spearman correlation analysis was used to determine the association of insulin sensitivity with echocardiographic measures of cardiac function. Insulin sensitivity was found to be significantly correlated with peak myocardial velocity during late diastole ($r = 0.89$, $p = 0.0419$), ratio between peak myocardial velocity in early and late diastole ($r = -0.92$, $p = 0.0263$), isovolumetric relaxation time ($r = -0.97$, $p = 0.0072$), and isovolumetric contraction time ($r = -0.90$, $p = 0.0374$). Due to the small sample size of this study, the relationship between insulin sensitivity and myocardial function requires further investigation.

TABLE OF CONTENTS

Chapter	Page
I. INTRODUCTION	1
II. REVIEW OF LITERATURE	3
2.1 Assessing insulin sensitivity and insulin resistance	3
2.1.1 Euglycemic hyperinsulinemic clamp	4
2.1.2 Frequently sampled intravenous tolerance test	4
2.1.3 Homeostatic model assessment	6
2.1.4 Oral challenge tests	7
2.1.5 Cresty neck score	8
2.2 Investigating cardiac function in horses	8
2.2.1 Echocardiographic modalities	11
2.2.2 Anatomic cardiac assessment	14
2.2.3 Assessment of systolic ventricular function	15
2.2.4 Assessment of diastolic ventricular function	17
2.2.5 Assessment of left atrial function	18
2.3 Link between metabolic syndrome and cardiovascular disease	19
2.3.1 Cardiac function in metabolic syndrome	19
2.3.2 Cardiovascular findings in ponies with equine metabolic syndrome	22
2.5 Scientific aims	23
III. METHODOLOGY	24
3.1 Research subjects	24
3.2 Determining insulin sensitivity	24
3.3 Echocardiography	25
3.4 Non-invasive blood pressure measurements	26
3.5 Statistical analysis	26

Chapter	Page
IV. RESULTS	28
4.1 Horses	28
4.2 Frequently sampled intravenous glucose tolerance testing.....	29
4.3 Echocardiography	29
4.4 Non-invasive blood pressure measurements.....	31
4.5 Statistical analyses	32
V. CONCLUSION	35
5.1 Insulin sensitivity.....	35
5.2 Myocardial function.....	36
5.2.1 Systolic function	37
5.3.2 Diastolic function.....	38
5.3 Myocardial hypertrophy	40
5.4 Other findings	41
5.5 Limitations.....	41
5.6 Conclusion.....	42
REFERENCES	43
APPENDICES	48

LIST OF TABLES

Table	Page
1. Cresty neck scoring system.....	9
2. Summary of testing performed.....	28
3. Summary characteristics for study population.....	29
4. Basal glucose and insulin concentrations, sensitivity index (S_I), and insulin resistance ($HOMA_{IR}$).....	30
5. Echocardiographic measurements.....	30
6. Non-invasive blood pressure measurements.....	32
7. Raw echocardiographic data for study horses.....	48
8. Raw blood pressure measurements for study horses.....	49
9. Raw correlation data.....	50

LIST OF FIGURES

Figure	Page
1. Schematic equations and parameters for the minimal model of glucose metabolism.....	6
2. A. Pulsed-wave tissue Doppler image of left ventricular free wall in a horse, showing representative myocardial velocity waves.....	12
B. Pulsed-wave tissue Doppler image of left ventricular free wall in a horse, showing representative time intervals.....	13
3. Relation between number of components of metabolic syndrome and measures of LV systolic and diastolic function.....	20
4. A. Representative left ventricular circumferential strain curve in a human patient with metabolic syndrome.....	21
B. Representative left ventricular longitudinal strain curve in a human patient with metabolic syndrome	21
5. Correlation between isovolumetric relaxation time (IVRT _m) and insulin sensitivity (S _I).....	33
6. Correlation between peak myocardial velocity during active atrial contraction in late diastole (A _m), and insulin sensitivity (S _I).....	33
7. Correlation between ratio of myocardial velocity during early (E _m) and late (A _m) diastole, and insulin sensitivity (S _I).....	33
8. Correlation between isovolumetric relaxation time cresty neck score (CNS) and insulin sensitivity (S _I).....	34
9. Correlation between isovolumetric contraction time (IVCT _m) and insulin sensitivity (S _I).....	34

LIST OF ABBREVIATIONS

2DST	two-dimensional speckle tracking echocardiography
a	at maximal atrial contraction
A	late diastolic peak measured by TDI, following the ECG P wave
Ac	active
AIR _g	acute insulin response to glucose
A _m	peak late-diastolic LV wall motion velocity at the time of atrial contraction
AoD	aortic (sinus) diameter
AR	aortic regurgitation
BP	blood pressure
CI	confidence interval
CV	cardiovascular
d	at the end of ventricular diastole
DI	disposition index
E	early diastolic peak measured by TDI, following the ECG R wave
E ₁	peak LV wall motion velocity during the phase of isovolumetric relaxation
ϵ_{cc}	circumferential strain
ECG	electrocardiogram
ECM	extracellular matrix
EHC	euglycemic hyperinsulinemic clamp
ELISA	enzyme-linked immunosorbent assay

ϵ_{LL}	longitudinal strain
E_m	early-diastolic peak LV wall motion velocity during the phase of rapid ventricular filling
E_m/A_m	ratio between peak radial wall motion velocities during early (E_m) and late (A_m) diastole
EMS	equine metabolic syndrome
EPSS	e-point septal separation
ET	left ventricular ejection time
ET_m	ejection time (measured with TDI)
FAC	fractional area change
FI	fasting insulin
FS	fractional shortening
FSIGTT	frequently sampled intravenous glucose tolerance test
G_b	basal glucose
GEZI	glucose effectiveness at zero insulin
GSC	global circumferential strain
H_0	null hypothesis
HDL	high density lipoprotein
$HOMA_\beta$	homeostatic model assessment of β -function
$HOMA_{IR}$	homeostatic model assessment of insulin resistance
HR	heart rate
I_b	basal insulin
ID	insulin dysregulation
IR	insulin resistance
$IVCT_m$	isovolumetric contraction time
$IVRT_m$	isovolumetric relaxation time
IVS	interventricular septum thickness
L	left (from left)
LA	left atrium

LAA	left atrial area
LAAmax	maximum left atrial area, (determined 1 frame before opening of the mitral valve)
LAAa	left atrial area at onset of active contraction (determined beginning of p wave)
LAAmin	minimum left atrial area (determined at closure of the mitral valve)
LAD	left atrial internal diameter
LA-RI _(area)	left atrial reservoir index determined by area
LA veloc	left atrial velocity
LOX	lysyl oxidase
LV	left ventricle
LVEF	left ventricular ejection fraction
LVPFW	left ventricular free wall thickness
LVMass	left ventricular mass (LVM)
LVIA	left ventricular internal area
LVIDd	left ventricular internal diameter in diastole
LVIDs	left ventricular internal diameter in systole
MetS	human metabolic syndrome
MOD	modified
MWT	mean wall thickness
NCEP	National Cholesterol Education Program
OSU	Oklahoma State University
p	at the onset of the P wave
Pa	passive
PAD	pulmonary artery diameter
PEP	left ventricular pre-ejection period
PEP _m	pre-ejection period (measured with TDI)
PW	pulsed-wave
R	correlation coefficient

RA	right atrium
rNCEP	revised National Cholesterol Education Program
RPA	right pulmonary artery
RR	relative risk
R-R interval	time elapsed between two successive R-waves of the QRS signal on the electrocardiogram
RV	right ventricle
RVIDd	right ventricular internal diameter in diastole
RVIDs	right ventricular internal diameter in systole
RWT	relative wall thickness
s	at the end of ventricular systole
S ₁	peak LV wall motion velocity during the phase of isovolumetric contraction
SD	standard deviation
S _G	glucose effectiveness index
S _I	insulin sensitivity index
S _m	positive systolic wave
SR	strain rate
SV	stroke volume
TDI	tissue Doppler imaging
TV	tricuspid valve
WHO	World Health Organization

CHAPTER I

INTRODUCTION

Metabolic syndrome (MetS) is a collection of risk factors that compromise vascular function resulting in subclinical and synergistic damage in a variety of organs. This syndrome develops in genetically susceptible individuals as a result of chronic inappropriate dietary intake and insufficient physical activity[1], and has become increasingly prevalent within the human population[2]. An individual with metabolic syndrome is defined by the National Cholesterol Education Program (NCEP) as having three or more of the following cardiovascular risk factors: central obesity (waist circumference ≥ 102 cm men, ≥ 88 cm women); increased triglycerides (≥ 150 mg/mL); diminished HDL cholesterol (men < 40 mg/dL, women < 50 mg/dL); systemic hypertension ($\geq 130/\geq 85$ mm Hg); and increased fasting glucose (≥ 110 mg/dL, ie insulin resistance)[1]. In 2004, this NCEP definition was revised (rNCEP) by lowering the threshold for fasting glucose to ≥ 100 mg/dL (in concordance with American Diabetes Association criteria for impaired fasting glucose), and including patients being treated for dyslipidemia, hyperglycemia, or systemic hypertension. In both humans and in animal models, metabolic syndrome is an established risk factor for cardiac disease[3-5].

Equine metabolic syndrome (EMS) is an increasingly recognized syndrome in horses, and is defined by a collection of risk factors for endocrinopathic laminitis, with insulin dysregulation a

central feature. Insulin dysregulation may be manifested by hyperinsulinemia; hyperglycemia; hypertriglyceridemia; and insulin resistance[6]. Other risk factors include generalized or regional adiposity, although this is not a necessary feature[7]. Diagnosis of EMS is based on history, clinical examination findings, and laboratory testing. Although the development of laminitis has remained the key clinical consequence of EMS, research has emerged linking EMS to cardiovascular changes, including hypertension and left ventricular hypertrophy [7, 8]. Due to overlaps between MetS and EMS, including insulin dysregulation, hypertension and cardiac hypertrophy, it is plausible that EMS may also be linked to cardiac dysfunction in horses.

In this study we aimed to determine if insulin sensitivity correlates with echocardiographic parameters of cardiac function. We hypothesized that decreased insulin sensitivity would not be correlated with changes in cardiac function, as measured with tissue Doppler imaging- and two-dimensional speckle tracking-derived indices of systolic and diastolic function.

CHAPTER II

REVIEW OF LITERATURE

2.1 *Assessing insulin sensitivity and insulin resistance*

Insulin dysregulation is an important aspect of both MetS and EMS. Insulin resistance is a physiologic state in which normal or increased concentrations of insulin are associated with an attenuated biologic response[9], and classically refers to impaired sensitivity to insulin mediated glucose disposal[10]. Insulin sensitivity refers to how sensitive the body is to the effects of insulin. Responses to insulin are usually measured as insulin sensitivity, and in this regard insulin resistance can be regarded as the inverse of low sensitivity of insulin receptors on the cell surface[11]. Yet, in addition to the sensitivity to insulin of glucose-utilizing tissues, carbohydrate disposal is also affected by the responsiveness of the pancreatic β -cells to glucose[12]. Thus, combined with transport of glucose into the cell, insulin resistance may also involve ineffectiveness resulting from various disruptions of intracellular glucose metabolism[11]. Multiple quantitative methods exist for assessing insulin sensitivity and insulin resistance in both horses and humans, including the euglycemic hyperinsulinemic clamp (EHC), minimal model assessment (frequently sampled intravenous glucose tolerance test, FSIGTT), homeostatic model assessment (HOMA)[13-15], and dynamic oral tests. The FSIGTT allows for assessment of the magnitude of insulin sensitivity, and in horses has been found to correlate well with the

euglycemic hyperinsulinemic clamp (EHC)[16], which is considered the gold standard for assessing insulin sensitivity in humans [17].

2.1.1 *Euglycemic hyperinsulinemic clamp*

In agreement with findings from human medicine, the euglycemic hyperinsulinemic clamp is considered the gold standard for measuring insulin resistance in horses and specifically measures insulin mediated glucose uptake under controlled conditions[13]. Following intravenous administration of glucose, there is an initial rapid phase of insulin release, which corresponds to the release of insulin that has already been synthesized and stored in secretory granules of pancreatic β -cells[18]. This first phase is then followed by a second phase in which there is secretion of both stored and newly synthesized insulin[18]. In the EHC, exogenous insulin is infused to maintain a constant plasma insulin concentration above fasting, whereas glucose is infused at varying rates to keep glucose within a fixed range[9]. The rate of glucose infusion at steady-state is an index of insulin action on glucose metabolism[9]. A high glucose infusion rate indicates effective insulin-induced glucose disposal and insulin sensitivity, whereas a low glucose infusion rate indicates tissue insulin resistance, with a value of $<7 \mu\text{mol/kg/min}$ used as an indicator of tissue insulin resistance in a general equine population[14]. Although this method is repeatable with a coefficient of variation of 14%[14], the test is labor-intensive and is limited to research settings.

2.1.2 *Frequently sampled intravenous glucose tolerance test*

The “minimal model” is a mathematical model of pancreatic insulin release and distribution to calculate insulin sensitivity, whereby computer modelling is performed to analyze the plasma glucose and insulin dynamics during a frequently sampled intravenous glucose tolerance test (FSIGTT)[17]. The minimal model is defined by two coupled differential equations with four model parameters (**Figure 1**)[15]. Plasma glucose dynamics in a single compartment are

described by the first equation, whereas insulin dynamics in a “remote compartment” are described by the second equation. Software allows the identification of unique model parameters to determine a best fit to glucose disappearance using the minimal model. As insulin causes glucose to decrease, and glucose causes insulin to increase, this method allows for the feedback loop to be mathematically analyzed to partition β -cell function and insulin resistance[13]. This model computes estimates of insulin resistance (S_I), glucose effectiveness (S_G), and β -cell function (Φ_1 and Φ_2) by curve fitting techniques; where S_I is the insulin sensitivity, Φ_1 is first phase of glucose kinetics (responsivity of β -cells to glucose), and Φ_2 is second phase of glucose responsivity[12]. Insulin sensitivity (S_I) is defined as the fractional glucose disappearance per insulin concentration unit (*ie* predicts glucose kinetics when the time-course is supplied)[17]. Glucose effectiveness (S_G) is defined as the ability of glucose *per se* to promote its own disposal and inhibit hepatic glucose production in the absence of an incremental insulin effect (*ie* when insulin is at basal concentrations)[15]. First phase responsivity (Φ_1) is the amount of insulin (per unit volume) that can be accounted for by an assumed injection of insulin (early insulin peak), per unit change in plasma glucose. It is assumed in the model that rate of rise of second-phase insulin secretion is proportional to the plasma glucose, such that second-phase responsivity (Φ_2) is the proportionality factor between glucose and the rate of rise[12].

Modification through the administration of an insulin bolus at a specified time point ensures that there is adequate insulin in the model to map glucose disappearance in response to insulin[13, 19, 20]. Horses with high S_I ($>1.5 \times 10^{-4}$ L/min/mU) are classified as insulin sensitive, whereas horses with low S_I ($<1 \times 10^{-4}$ L/min/mU) are classified as having tissue insulin resistance[21]. Insulin sensitivity derived from the insulin modified FSIGTT is strongly correlated with results from the EHC ($r = 0.86$)[22], and this method is often considered less labor-intensive than the

EHC. Software developed for minimal model analysis will calculate sensitivity index in addition to providing an estimate of insulin resistance (I_R) using HOMA[23].

$$dG(t)/dt = -[p_1 + X(t)] G(t) + p_1 G_b$$

$$dX(t)/dt = -p_2 X(t) + p_3 [I(t) - I_b]$$

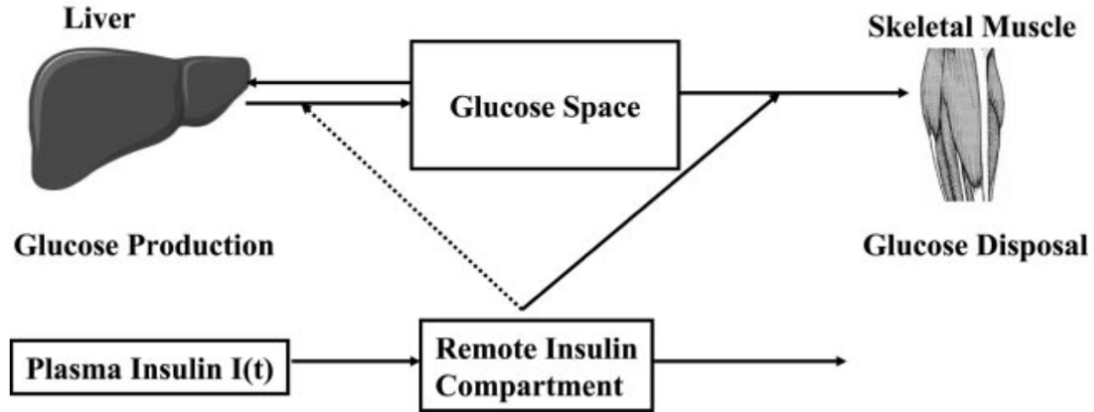


Figure 1. Schematic equations and parameters for the minimal model of glucose metabolism. Differential equations describing glucose dynamics [$G(t)$] in a mono-compartmental “glucose space” and insulin dynamics in a “remote compartment” [$X(t)$] are shown at the top. Glucose leaves or enters its space at a rate proportional to the difference between plasma glucose concentration, $G(t)$, and the basal fasting insulin concentration, G_b . In addition, glucose also disappears from its compartment at a rate proportional to insulin concentrations in the “remote” compartment [$X(t)$]. In this model, t = time; $G(t)$ = plasma glucose at time t ; $X(t)$ = insulin concentration in “remote” compartment at time t ; G_b = basal plasma glucose concentration; I_b = basal plasma insulin concentration; $G(0) = G_0$ (assuming instantaneous mixing of the IV glucose load); p_1 , p_2 , p_3 , and G_0 = unknown parameters in the model that are uniquely identifiable from FSIGTT; glucose effectiveness = p_1 ; and insulin sensitivity = p_3/p_2 . From: “Current approaches for assessing insulin sensitivity and resistance in vivo: advantages, limitations and appropriate usage”. Muniyappa *et al. Am J Physiol Metab* 2007;294:E15-E26.

2.1.3 Homeostatic model assessment

One-sample tests have been developed for the screening of metabolic syndrome in humans and other animals, although these provide a much less precise means of assessing insulin resistance than the EHC or minimal model analysis. The homeostasis assessment model (HOMA) allows values for insulin resistance and β -cell function (expressed as a percentage of normal) to be obtained if simultaneous fasting plasma glucose and fasting insulin concentrations are known[13].

Although the previously discussed models measure stimulated insulin resistance, HOMA gives only estimates of basal insulin resistance (HOMA_{IR}) and β -cell function (HOMA_{β})[13]. An estimate of insulin resistance is provided through the formula $\text{HOMA}_{\text{IR}} = \text{fasting insulin } (\mu\text{U/mL}) \times \text{fasting plasma glucose } (\text{mmol/L})/22.5$. In humans, estimates of insulin resistance derived from HOMA_{IR} are reported to correlate well with estimates derived from the EHC ($r = 0.88$), and to the fasting insulin (FI) concentration ($r = 0.81$)[24]. However, this model was also found to have low precision of estimates (coefficient of variation 31% for insulin resistance) [13, 24]. An estimate of basal β -cell function is given by $\text{HOMA}_{\beta} = (20 \times [\text{insulin}])/[\text{glucose}] - 3.5$ [25]. A recent study in horses comparing the results of proxy tests found that HOMA_{β} and FI correlated well with results of EHC, with cut-offs of >147 and $>9.5 \mu\text{IU/mL}$ respectively to diagnose insulin resistance, with CVs $\leq 25.3\%$ [25]. That study also concluded there was no advantage to using HOMA_{β} over FI[25]. Compared with EHC, HOMA_{β} was found to have a sensitivity and specificity for diagnosing insulin resistance of 79% and 96%[25]. Compared with EHC, FI was found to have a sensitivity and specificity of 91% and 85% for diagnosing insulin resistance[25]. When compared with a combined glucose-insulin test, fasting insulin has been found to correlate well for the diagnosis of insulin dysregulation in horses, with a sensitivity and specificity of 63.4% and 87.2%, respectively, using a cut-off of $5.2 \mu\text{mol/L}$ [26].

2.1.4 *Oral challenge tests*

Oral glucose[27] and sugar tests[28] involve the administration of a standardized dose of a simple sugar source (glucose powder or corn syrup) following a period of fasting. Blood glucose and insulin concentrations are measured pre- and post-administration at a specified time point (120 minutes following glucose, or 60 to 90 minutes following corn syrup[6, 14]). An insulin concentration above a certain cut-off is used to diagnose insulin dysregulation, with the specified cut-off varying for carbohydrate dosages, and insulin assay used[6, 14]. These tests are simple to

perform and useful for the diagnosis of insulin dysregulation in individual horses, however they do not provide a quantitative measure of insulin sensitivity[6].

2.1.5 *Cresty neck score*







The presence of central obesity above a certain threshold is one of the possible criteria used to diagnose metabolic syndrome in humans, with regional fat deposition more predictive of metabolic disease than overall body fat[29]. Similar to central obesity in humans, deposition of adipose tissue along the crest of the neck in horses ('cresty neck') has been associated with insulin resistance and an increased risk for laminitis[30, 31]. A scoring system has been described for assessment of apparent neck crest adiposity ("cresty neck score", CNS) in horses and ponies[32] (**Table 1**). In ponies, cresty neck scores have been found to correlate well with basal serum insulin ($r = 0.59$), and those with a cresty neck were 18.9x more likely to be hyperinsulinemic (serum insulin ≥ 30 mU/L)[32]. The presence of a cresty neck is associated with insulin resistance and an increased risk for laminitis in both horses and ponies[28, 29, 31]. In a more recent study, ponies with a CNS of ≥ 3 were 5x more likely to have insulin dysregulation than those with a CNS < 3 , regardless of body condition score, as evaluated using post-prandial serum insulin concentrations following an oral glucose test[34].

2.2 *Investigating cardiac function in horses*

In horses, echocardiography remains the gold standard method for noninvasive evaluation of cardiac chamber dimensions, structure and function. Echocardiography enables the investigation of heart murmurs to determine their source (physiological vs pathological) and clinical relevance; screening for endocarditis or pericarditis; the detection of pulmonary hypertension; and changes in chamber size and wall thickness[35]. M-mode and two-dimensional (2D) real-time echocardiography and various Doppler modalities, including continuous wave (CW) Doppler, pulsed-wave (PW) Doppler and color flow Doppler, provide the basis for comprehensive

evaluation of internal cardiac structures, chamber dimension, blood flow characteristics, and mechanical function of the equine heart[35].

Table 1. Cresty neck scoring system with illustrations of individual cresty neck scores. From: “Apparent adiposity assessed by standardised scoring systems and morphometric measurements in horses and ponies”. Carter RA *et al. The Veterinary Journal* 2009;179:204-210.

Score	Description	Visual illustration
0	No visual appearance of a crest (tissue apparent above the <i>ligamentum nuchae</i>). No palpable crest.	
1	No visual appearance of a crest, but slight filling felt with palpation.	
2	Noticeable appearance of a crest, but fat deposited fairly evenly from poll to withers. Crest easily cupped in one hand and bent from side to side.	
3	Crest enlarged and thickened, so fat is deposited more heavily in middle of the neck than toward poll and withers, giving a mounded appearance. Crest fills cupped hand and begins losing side to side flexibility.	
4	Crest grossly enlarged and thickened, and can no longer be cupped in one hand or easily bent from side to side. Crest may have wrinkles/creases perpendicular to topline.	
5	Crest is so large it permanently droops to one side.	

Newer techniques such as 2D speckle tracking (2DST) and tissue Doppler imaging (TDI) allow assessment of regional and global ventricular function, and quantitative assessment of myocardial wall motion velocity, deformation (strain, ϵ), deformation rate (strain rate, SR), displacement, and rotation in longitudinal, radial and circumferential imaging planes[35, 36]. These modalities are purported to allow for a more sensitive means of assessing regional or global myocardial function in horses.

Deformation analyses (strain and strain-rate imaging) allow discrimination between active and passive myocardial tissue movement. Myocardial strain and strain rate describe the shortening and lengthening of myocardium and reflect tissue compressibility[37]. Strain (positive or negative) represents the amount of deformation, and is usually expressed in %[38]. Relative to the original length of a myocardial segment, thickening of a given segment is represented by positive strain, whereas negative strain represents shortening[38]. Strain rate (SR) is the rate by which the deformation occurs (deformation or strain per time unit), with unit s^{-1} [38]. The local rate of deformation or strain per time unit equals velocity difference per unit length:

$$\epsilon = \frac{\Delta\epsilon}{\Delta t} = \frac{(\Delta L/L_0)}{\Delta t} = \frac{(\Delta L/(\Delta t))}{L_0} = \frac{\Delta V}{L_0},$$

where ϵ = strain, L_0 = baseline length, L = instantaneous lengths at the time of measurement, t = time, and ΔV is the velocity gradient of the studied segment[38].

Strain represents the total systolic shortening, and thus is very afterload-dependent, whilst peak systolic strain rate is more closely related to contractility[36]. Circumferential strain represents the change in length of the myocardium (shortening in systole, represented as a negative strain value) along the circumferential axis of the ventricle (on a short axis view[39]). In reality, the myocardium deforms simultaneously in three-dimensions. Global circumferential strain is

averaged from 12 regional segments across 2 parasternal short axis views, 6 segments at the mitral valve level and 6 segments at the papillary muscle level[39]. For assessment of regional myocardial dysfunction, strain and SR imaging (deformation analysis) are considered more sensitive than wall motion analysis (velocity and displacement)[38].

2.2.1 Echocardiographic modalities

2D Echocardiography The 2D echocardiogram generates a topographic image by sweeping an ultrasound beam across the heart, and allows assessment of cardiac anatomy, detection of macroscopic structural lesions, subjective evaluation, and measurement of chamber and vessel dimensions, and evaluation of left atrial (LA) and left ventricular (LV) function[40].

M-mode echocardiography In M-mode echocardiography, the movement of cardiac structures (vertical axis) is displayed over time (horizontal axis), which can be used to quantify cardiac anatomy and myocardial function, and is especially useful for visualizing rapidly vibrating structures such as regurgitant valve lesions due to the high sampling rate[40].

Doppler echocardiography The Doppler effect describes the change in frequency of reflected sound waves from emitting sound waves when the reflecting object is in motion. Doppler echocardiography utilizes this principle to measure the direction and velocity of red blood cells moving through the heart, with the information displayed as spectral tracing[40]. When using Doppler, parallel alignment with the direction of movement of the target is critical as excessive angle of interrogation results in underestimation of velocities, thus this modality may only be accurately used for blood moving parallel to the ultrasound beam[40]. Pulsed-wave (PW) Doppler enables measurement of direction and velocity of red blood cells within a discrete area of the heart[40].

enable evaluation of general cardiac structure and function, Tissue Doppler imaging (TDI) allows assessment of myocardial function through quantification of myocardial wall motion velocity[36]. It can be used to evaluate global and regional myocardial systolic and diastolic function, and to quantify right ventricular and left atrial function[39], and has enabled the detection of subtle systolic and diastolic myocardial dysfunction in human patients. Signals representing tissue velocity can be displayed as spectral tracings (PW TDI)[40]. As for the other Doppler-based modalities, velocity measurements obtained by TDI depend on the angle of interrogation and may only be performed in a single dimension[40].

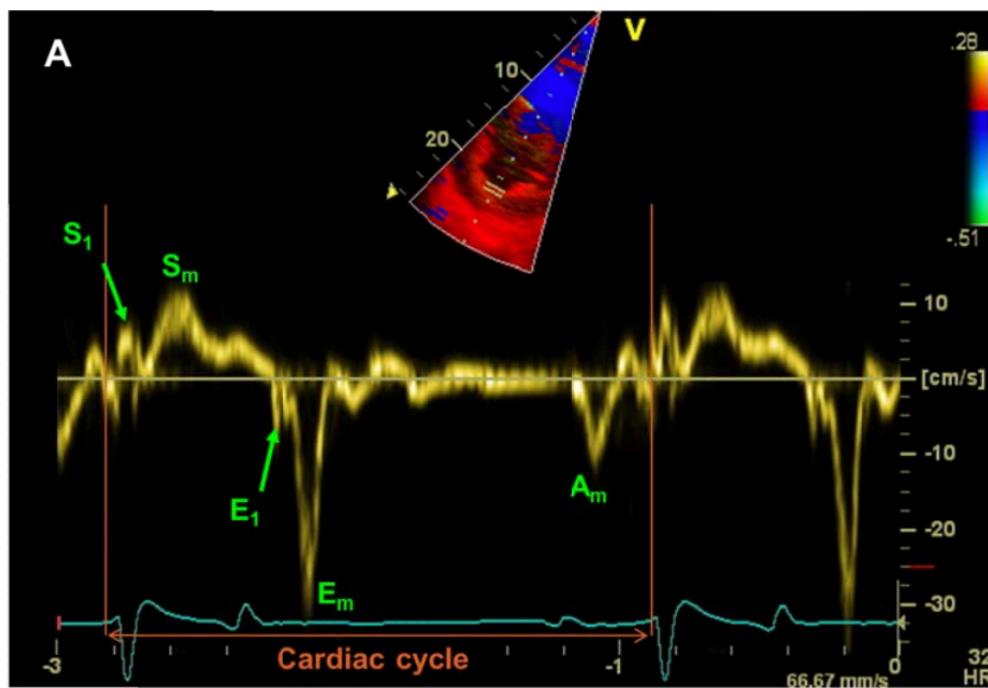


Figure 2A. Horse: Pulsed-wave tissue Doppler image of the left ventricular free wall, recorded at the level of the chordae tendinae, showing representative myocardial velocity waves. The start and end of the cardiac cycle are represented by the orange vertical lines. The horizontal scale of the spectral tracing indicates the time in seconds whilst the vertical scales indicate the velocity in centimeters per second. The sample volume is in a fixed position relative to the transducer. S_1 , peak velocity during isovolumic contraction; S_m , peak velocity during ejection; E_1 , peak velocity during isovolumic relaxation; E_m , peak velocity during early diastole; A_m , peak velocity during late diastole. From: “Echocardiographic assessment of left ventricular function in healthy horses and in horses with heart disease using pulsed-wave tissue Doppler imaging”. Koenig *et al. J Vet Intern Med* 2017;31:556-567.

The TDI signal has three peaks corresponding to myocardial tissue velocities: a positive systolic peak (S_m), which represents myocardial contraction; and two negative diastolic peaks, which represent early diastolic myocardial relaxation (E_m) and active atrial contraction in late diastole (A_m)(see **Figure 2A**). The TDI signal also allows for assessment of isovolumetric relaxation time ($IVRT_m$), and isovolumetric contraction time ($IVCT_m$)[39] (**Figure 2B**). Isovolumic contraction time is defined as the time period from the mitral valve closure to the start of ejection – as such there is no volume change and hence no deformation during this phase[36]. It is during this phase however that the period of most rapid rise in pressure occurs[36]. The duration of $IVCT_m$ is shortened by the rate of force development (a function of preload and contractility), but it is also shortened by increased HR, and affected by both preload and afterload[36]. Systolic ejection velocity (S') follows $IVCT_m$ and precedes $IVRT_m$ [42].

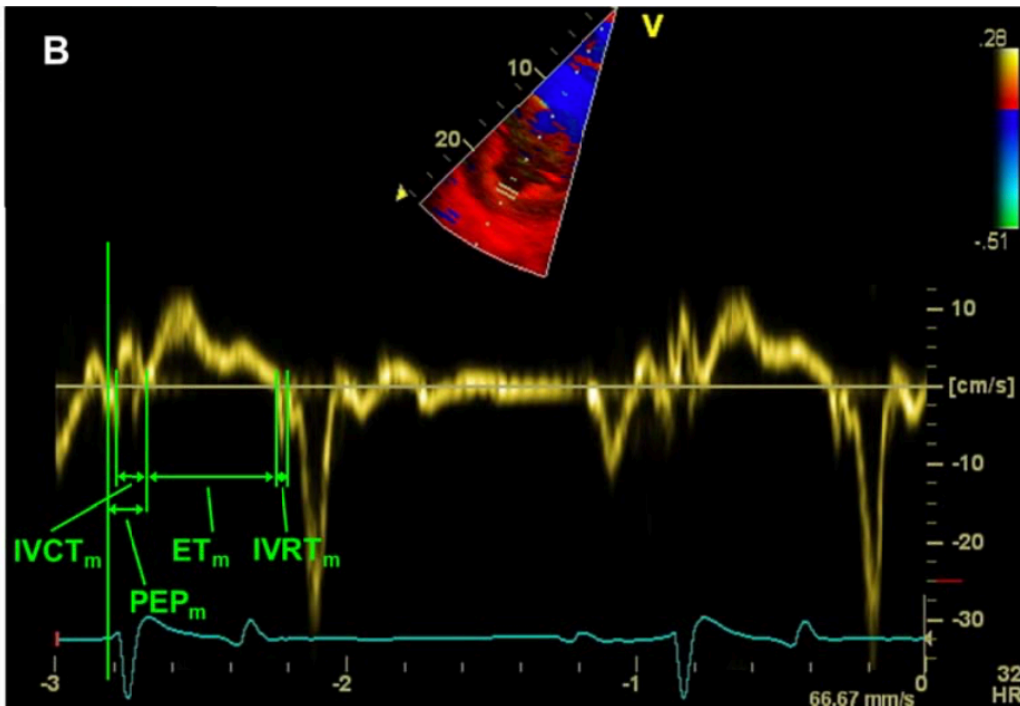


Figure 2B. Horse: Pulsed-wave tissue Doppler image of the left ventricular free wall, recorded at the level of the chordae tendinae, showing representative time intervals. The horizontal scale of the spectral tracing indicates the time in seconds. The sample volume is in a fixed position relative to the transducer. $IVCT_m$, time from onset of S_1 to onset of S_m ; PEP_m , time from onset of QRS until onset of S_m ; ET_m , time from onset to end of S_m ; $IVRT_m$, time from onset of E_1 to onset of E_m . See **Figure 2A** for remainder of legend. From: “Echocardiographic assessment of left ventricular function in healthy horses and in horses with heart disease using pulsed-wave tissue Doppler imaging”. Koenig *et al. J Vet Intern Med* 2017;31:556-567.

Reference intervals for PW TDI variables of radial LV wall motion have been established in horses[43]. The use of TDI for regional quantification of radial left ventricular wall motion in healthy horses has been reported[42, 43], with measurement variabilities very low (CV <5%) to low (CV 5-15%) for most variables[45]. For most variables, within-day interobserver variability as well as between-day interobserver and intra-observer variabilities were low to moderate (CV 16-25%)[45]. All PW TDI variables of systolic LV function showed very low to low variability, however some of the variables of LV diastolic and LA function, including E_m/A_m ratio and $IVRT_m$, showed moderate to high (CV >25%) variability. In a study of 10 healthy horses, the authors reported that determination of TDI measurements of velocity, strain rate, and strain were feasible for each horse, however left ventricular free wall deformation could not be consistently measured[44]. The authors found a significant correlation ($r = 0.45 - 0.89$) between TDI-based time measurements and M-mode and pulsed-wave Doppler measurements[44].

Two-dimensional speckle tracking 2DST is based on conventional 2DE cine-loop recordings and is independent of the Doppler principle[40]. 2DST allows tracking of myocardial motion throughout the entire cardiac cycle through the analysis of greyscale speckles as they move during contraction and relaxation[40]. The advantage of 2DST over TDI is that it offers a Doppler-independent approach to the measurement of ϵ and SR, and due to its independence from the angle of interrogation, simultaneous measurements of ϵ and SR may be obtained in two-dimensions[40].

2.2.2 Anatomic cardiac assessment

2D and M-mode echocardiography provide the basis for assessment of chamber and great vessel dimensions. Quantification of left atrial and left ventricular internal dimensions, wall thickness, and size of the great vessels during different cardiac phases are obtained using linear measurements, area measurements, or volumetric estimates based on 2D and M-mode

echocardiography[35]. Due to the complex geometric shape of the right heart and the effect of transducer placement and imaging plane on the apparent internal dimensions of the right atrium (RA) and right ventricle (RV), objective quantification of these chambers is difficult, thus subjective assessment in multiple planes remains important[35].

2.2.3 *Assessment of systolic ventricular function*

In general, traditional indices of global systolic ventricular function are influenced by preload, afterload, heart rate and rhythm and do not reflect contractility[35]. Echocardiography-derived strain and strain rate imaging provide additional indices of regional and global ventricular function[36].

2D Ejection phase indices Measurements of LV dimensions provide the basis for the calculation of 2D ejection phase indices. Left ventricular ejection fraction (EF%) has traditionally been the standard index of LV systolic function, and is based upon the use of geometric estimates of LV volumes to enable calculation ($EF\% = \text{stroke volume} / \text{LV end-diastolic volume} \times 100$)[35]. Objective evaluation of LV function is traditionally based on M-mode measurements such as fractional shortening and wall thickening[46, 47]. In horses, the LV fractional shortening (FS%) is the most commonly used index of LV systolic function as it is easily calculated from M-mode recordings of LV internal short-axis dimensions, and provides an approximation of EF%[35]. Fractional shortening is given by $FS\% = (LVIDd - LVIDs) / LVIDd \times 100$, where LVID is the LV internal diameter, measured at peak-systole (time at which LV internal lumen is narrowest) and end-diastole (onset of the ECG QRS complex). Although the LV contracts simultaneously in all 3 dimensions, FS% only represents relative shortening in a single dimension.

In a study investigating ventricular function in horses exposed to lasalocid (Decloedt *et al*, 2012)[48], TDI and 2DST measurements were significantly correlated with FS% ($r = 0.33 -$

0.88). That study also found that compared with control horses, of those horses classified as having mild myocardial damage (as measured by cardiac troponin I, a biomarker of myocardial damage) only 1/15 horses had a decreased FS, whereas 8/15 horses had decreased TDI or 2DST measurements, suggesting that TDI and 2DST may enable detection of more subtle myocardial dysfunction compared with FS[48].

Systolic time intervals Left ventricular pre-ejection period (PEP, measured from M-mode images of Ao valve motion), LV ejection time (ET, measured from Doppler tracings Ao blood flow), and LV PEP-ET ratio (PEP/ET) serve as complementary indicators of LV function, and are independent of ventricular shape and geometry[40]. It is important to note however that these indices are variably influenced by heart rate and loading conditions[40]. The use of TDI for measurement of systolic time intervals overcomes the challenge of clear identification of the onset and end of ejection on M-mode and Doppler tracings[40].

Tissue velocity, strain, and strain rate Reduced myocardial tissue velocity during systole (S_m) and prolonged $IVCT_m$ provide evidence of subclinical LV systolic dysfunction. Duration of $IVCT_m$ can be used as a measure of contractility, as increased (mean) rate of pressure rise will reduce the $IVCT_m$ (although it must be remembered that it is preload dependent)[36]. TDI has allowed detection of systolic (and diastolic) LV dysfunction in horses with nutritional and toxic myocardial damage[46, 47].

Strain and strain rate imaging have also been used to detect subclinical systolic dysfunction, and allow for objective assessment of myocardial performance. Systolic strain (ϵ), a measure of deformation of a myocardial segment and expressed as a percentage of change from its original dimension, provides an analog of regional ejection fraction (%EF) for normal myocardium[40]. Systolic strain rate (SR), the rate of deformation and the temporal derivative of ϵ , reflects regional contractile function[40]. In human medicine, ϵ and SR have been used for diagnosing subclinical

myocardial disease, and for differentiating hypertrophy caused by hypertension or cardiomyopathy.

2.2.4 *Assessment of diastolic ventricular function*

Diastolic left ventricular function and filling pressures are commonly assessed in humans and small animals using Doppler-derived transmitral flow velocities and tissue Doppler analyses of mitral annular or myocardial velocities[35]. In horses however, optimal alignment with blood flow and consistent placement of the sample volume relative to the mitral valve means that determining transmitral flow velocities using PW Doppler is both challenging and unreliable due their size[33, 38, 48-50]. Diastolic dysfunction may be suspected when there is marked decrease or reversion of the ratio between the early diastolic (E wave) and the late-diastolic (A wave) transmitral blood flow velocity (E/A ratio)[49].

TDI has shown to be a promising tool for detection of LV diastolic dysfunction in horses[33, 41, 43, 47, 51, 52]. This modality provides additional indices that are easier to obtain and helpful for assessing LV diastolic myocardial function in horses, including velocity-based (eg ratio between the peak radial wall motion velocities during early diastole (E_m wave) and during late diastole (A_m wave), termed E_m/A_m ratio) and time-interval based ($IVRT_m$) indices[38, 41-43, 47]. Reduced E_m and A_m , and prolonged $IVRT_m$ provide evidence of subclinical LV diastolic dysfunction. In humans, $IVRT_m$ is ≤ 70 msec in normal subjects and is prolonged in patients with impaired LV relaxation but normal LV filling pressures[42]. In the presence of increased left atrial pressure, $IVRT_m$ shortens and its duration is inversely related to LV filling pressures in patients with cardiac disease[42].

TDI and 2DST have been used to confirm diastolic dysfunction in horses with atypical myopathy[54]. In that study, horses with atypical myopathy had a longer duration of $IVRT_m$ with

normal ejection time, indicating impaired LV relaxation[54]. Diastolic dysfunction was also evidenced by decreased diastolic myocardial velocities, with decreased E_m and a decreased E_m/A_m ratio[54]. Right ventricular index of myocardial performance (RIMP, where $RIMP = (IVRT_m + IVCT_m)/E_m$) is a TDI-derived index of global RV performance that has been used in humans, where $RIMP > 0.54$ indicates RV dysfunction[53]. To the author's knowledge however, this index has not yet been validated in horses.

2.2.5 *Assessment of left atrial function*

Left atrial function is impaired in atrial fibrillation, hence investigation of LA function is an important part of the echocardiographic examination of horses experiencing AF. The use of 2DE, transmitral Doppler flow velocity profiles, and analysis of LA wall motion by TDI and 2DST allows for assessment of left atrial size and mechanical function in horses[40, 50]. 2DE variables used in horses include LA area and LA fractional area change [50]. Following conversion from AF to sinus rhythm in horses, persistent LA contractile dysfunction can be detected and is likely attributable to AF-induced atrial remodeling[38, 49, 54, 55]. In a study by Schwarzwald *et al* (2007), the authors found echocardiographic evidence of left atrial mechanical dysfunction following conversion of AF to sinus rhythm in 5 horses[51]. In that study, 2D indices of LA contractile function (active LA FAC and active/total LA AC) and the index of LA reservoir function were significantly decreased 24 hours after conversion compared to normal horses[51]. That study also found significant prolongation of TDI-derived systolic time intervals 24 hours following conversion compared to normal horses, further supporting the persistence LA contractile dysfunction in that group[51].

Both TDI[42, 43, 46, 47, 49, 52, 56] and 2DST[46, 47, 52, 56-59] have been utilized and validated in horses. These studies have shown that radial wall motion velocities and systolic time intervals measured by TDI as well as ϵ and SR measured by 2DST can reliably be used to

characterize LV wall motion and to assess LV systolic and diastolic function in horses[38, 46, 47, 52].

2.3 *Link between metabolic syndrome and cardiovascular disease*

The link between MetS and the development of more serious cardiac disease is well established in humans[3, 5]. Using definitions outlined by both the 2001 National Cholesterol Education Program (NCEP) and 2004 revised National Cholesterol Education Program (rNCEP), MetS was associated with increased risk of CV disease (RR 2.35; 95% CI 2.02 to 2.73), CV disease mortality (RR: 2.40, 95% CI 1.87 – 3.08), all-cause mortality (RR: 1.58; 95% CI: 1.39 to 1.78), myocardial infarction (RR: 1.99; 95% CI: 1.61 to 2.46), and stroke (RR: 2.27; 95% CI: 1.80 to 2.85)[62]. Humans with MetS are at twice the risk of developing cardiovascular disease within 5 to 10 years subsequent to diagnosis, as are those individuals without MetS[63].

2.3.1 *Cardiac function in metabolic syndrome*

A significant linear relationship has been found between a number of components of MetS and TDI-derived measures of LV systolic and diastolic function (see **Figure 3**)[37]. Patients with MetS had decreases in: peak velocity of active mitral filling (A); peak early diastolic myocardial velocity (E_m); ejection fraction (EF%); peak systolic myocardial velocity (S_m); and less negative strain (ϵ) and strain rates (SR)[37]. Patients with MetS had reduced systolic and diastolic function even in the absence of LV hypertrophy ($p < 0.001$)[37].

Speckle Tracing Echocardiography (2DST) has also been used to investigate systolic function in patients with MetS, with individuals with MetS having significantly lower (ie less negative) LV circumferential (ϵ_{CC}) and longitudinal (ϵ_{LL}) strain (see **Figures 4A, 4B**)[64]. Following multivariate analysis, MetS was associated with less circumferential myocardial shortening (as

indicated by less negative ϵ_{CC} ; and MetS and LV mass were significantly associated with less longitudinal myocardial shortening (as indicated by less negative ϵ_{LL})[64].

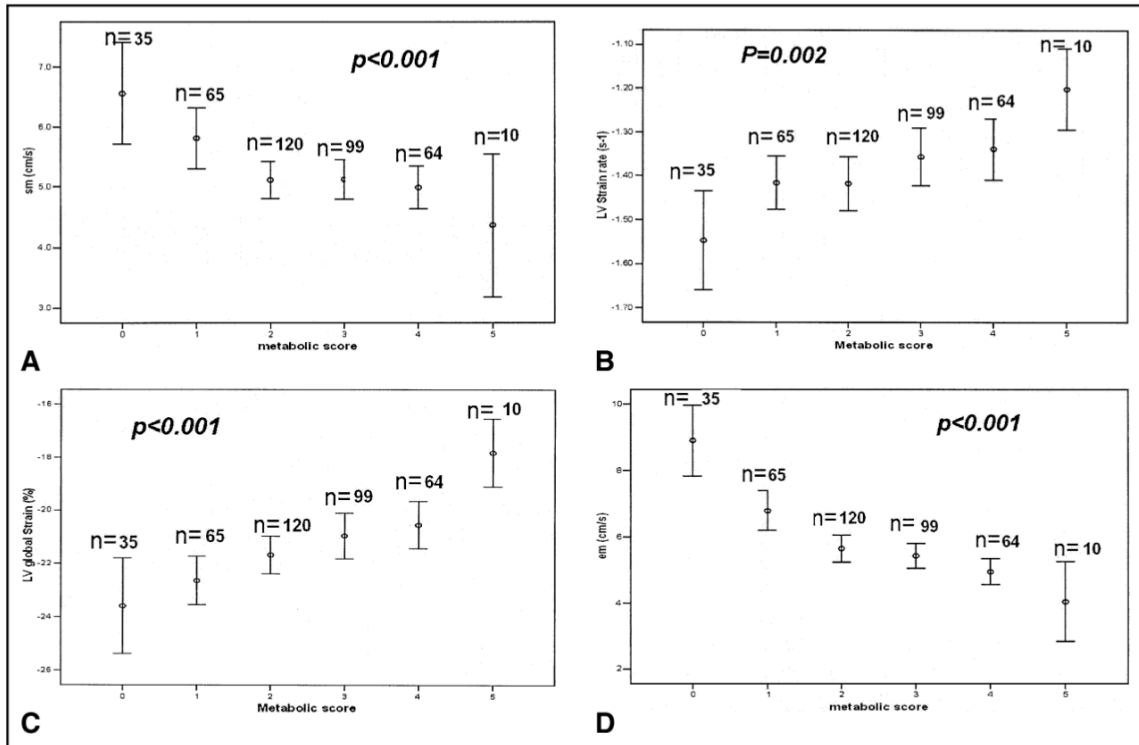


Figure 3. Relation between number of components of MetS and systolic (S_m) myocardial velocity (A), LV strain rate (B), LV global strain (C), and diastolic (E_m) myocardial velocity (D) (mean \pm SD, analysis of variance with 95% confidence intervals). From: “Myocardial and vascular dysfunction and exercise capacity in the metabolic syndrome”. Wong CY, *et al. Am J Cardiol.* 2005;96:1686-1691.

Even in patients with normal LV EF% (a measure of LV systolic function), patients with MetS have significantly decreased mean systolic strain, peak systolic strain rate, and peak early diastolic strain rate compared with control subjects[63], suggesting that these parameters may provide an earlier and more sensitive measure of myocardial dysfunction than traditional measures of ventricular function. The degree of myocardial dysfunction, as measured by decreases in mean systolic strain and peak early systolic strain rate, also increased with the number of metabolic abnormalities[63].

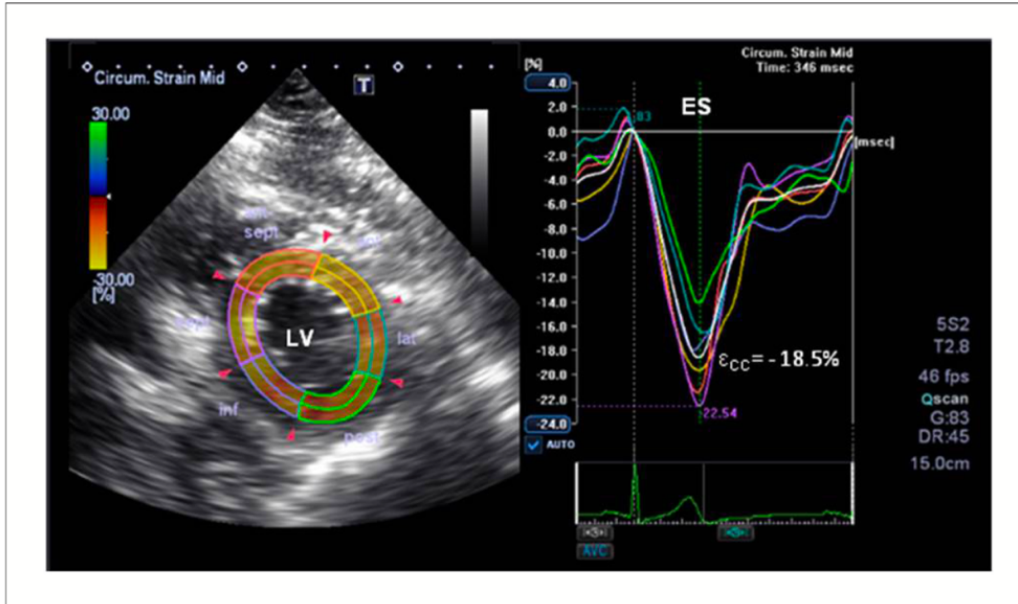


Figure 4A. Representative LV ϵ_{CC} curve from a human patient with MetS. Different colors depict different myocardial segments. The white strain curve represents the global circumferential peak strain. ES: end-systole; ϵ_{CC} circumferential strain; LV left ventricle. From: “Metabolic syndrome and reduced myocardial function”. Almeida *et al. Arq Bras Cardiol* 2014;102(4):327-335.

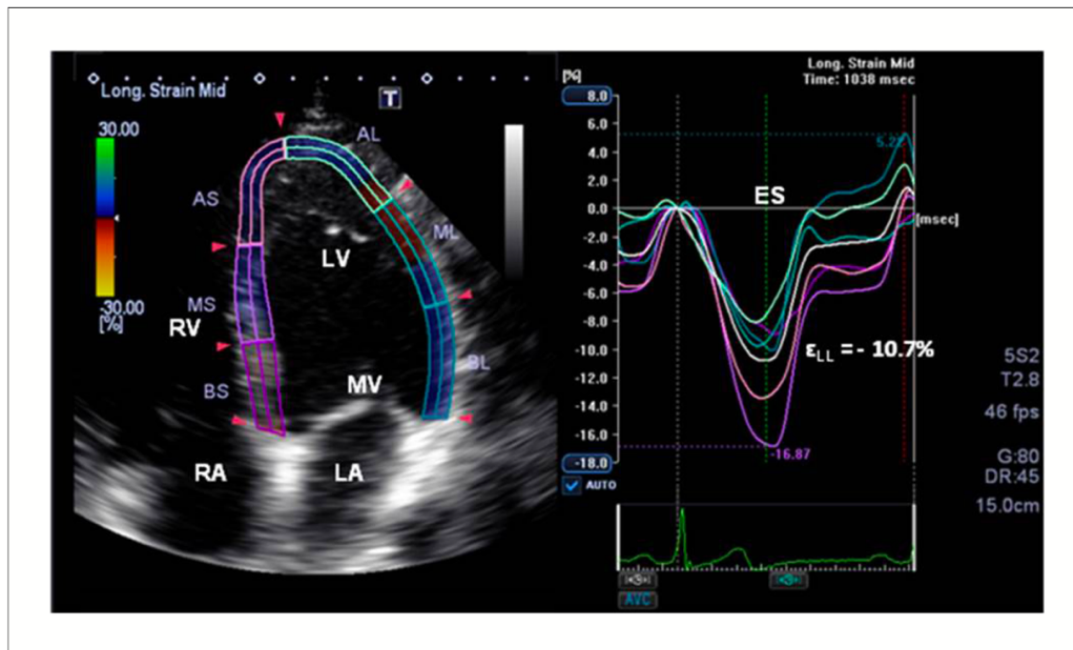


Figure 4B. Representative LV ϵ_{LL} curve from a human patient with MetS. Different colors depict different myocardial segments. The white strain curve represents the global longitudinal peak strain. ES: end-systole; ϵ_{LL} longitudinal strain; LV left ventricle; LA left atrium; RV: right ventricle; RA: right atrium; MV: mitral valve. From: “Metabolic syndrome and reduced myocardial function”. Almeida *et al. Arq Bras Cardiol* 2014;102(4):327-335.

Associations have also been found between metabolic disease and hypertension, changes in cardiac autonomic function, and ventricular wall thickness. Compared with control subjects, patients with one or more metabolic abnormalities (central obesity, fasting hyperglycemia, hypertension, hypertriglyceridemia, or low HDL cholesterol) have been found to have a lower standard deviation of R-R interval, suggesting that changes in cardiac autonomic function may precede the development of MetS in pre-disease subjects[66]. Patients with MetS have also been found to have significant increases in systolic and diastolic blood pressures, and significant linear increases in ventricular (septal and posterior) wall thickness and LV mass index compared with controls[63].

Cardiac changes have also been identified in murine models of MetS. In mice with diet-induced MetS, alteration in expression of remodeling enzymes resulted in increased amounts of cross-linked collagen in cardiac tissue and diastolic dysfunction[65]. In the study by Zibadi *et al* (2009), the authors investigated the effect of MetS on gene expression of cardiac ECM-modifying enzymes that catalyze the formation of collagen cross-linking, including lysyl oxidase (LOX). In that study, the authors found increased LOX activity, and increased cardiac cross-linked collagen compared with controls, with the fibrotic response coinciding with a marked increase in end-diastolic pressure, increased left ventricular stiffness, and impaired diastolic filling pattern[65].

2.3.2 *Cardiovascular findings in ponies with equine metabolic syndrome*

A study by Heliczzer *et al* (2017)[8] investigated cardiovascular findings in ponies diagnosed with EMS. The authors found correlations between resting insulin concentration and relative wall thickness; and that compared with healthy controls, ponies with EMS had higher mean \pm SD HR (44.5 ± 7.5 bpm vs 38.6 ± 6.8 pm) and median left ventricular wall thickness (2.0 cm vs 1.8 cm)[8]. These results suggest an association between EMS and myocardial hypertrophy that requires further investigation in horses.

Compared with control, laminitis-prone ponies at pasture have been found to have significantly higher insulin resistance and mean blood pressure during the summer months, but not during winter[7]. In that study, insulin sensitivity was calculated with proxies derived from basal serum insulin and plasma glucose. Mean blood pressures during summer in laminitis-prone ponies were found to be (median [interquartile range], 89.6 mm Hg [78.3 to 96.9 mm Hg]), compared with control ponies (76.8 mm Hg [69.4 to 85.2 mm Hg]). This study suggests that further investigation of blood pressure in EMS is warranted.

2.5 *Scientific aims*

Whilst the relationship between human metabolic syndrome and cardiac dysfunction is well established, to the author's knowledge, no studies have yet investigated the relationship between EMS and TDI- and 2DST-derived indices of cardiac function in horses. Although diagnosis of EMS is complex, degree of insulin sensitivity may be established through quantitative testing. The objective of our study was to investigate the relationship between insulin sensitivity and echocardiographic parameters of cardiac function.

Our hypothesis (H_0) was that insulin sensitivity would not be correlated with changes in cardiac function, as measured with TDI- and 2DST-derived indices of systolic and diastolic function.

CHAPTER III

METHODOLOGY

3.1 *Research subjects*

The study was performed with the approval of the Oklahoma State University (OSU) Institute for Animal Care and Use Committee. Horses were purchased from a local dealer based on their metabolic phenotype. Each horse was scored based on body condition[68] and given a cresty neck score[32]. Horses were weighed, had ages estimated based on dentition, and underwent basic physical examinations, and screening echocardiography. Horses with serious underlying cardiac disease were eliminated. Two horses from the OSU teaching herd were used for parts of the experiment. During the study period, horses were maintained at pasture with free choice access to grass hay. Horses 1-6 underwent screening for *Streptococcus equi* subsp. *equi* (nasal wash qPCR) and had blood collected for plasma biochemistry and complete blood count.

3.2 *Determining insulin sensitivity*

Insulin sensitivity was determined using the insulin-modified frequently sampled intravenous glucose tolerance test. Horses were stabled in pairs to minimize stress, and each horse was fasted for 10 hours. Both jugular veins were clipped, aseptically prepared, and infiltrated with 2% lidocaine. An 18G 1.88-inch catheter¹ was placed in the right jugular vein for glucose and insulin

¹ BD Insyte, Becton Dickinson Infusion Therapy Systems Inc, Sand, Utah

administration, and a 14G 3.5-inch catheter² was placed in the left jugular vein for sample collection. Samples were taken for basal glucose and serum insulin. The insulin-modified FSIGTT was performed as outlined by Toth *et al* (2009)[69]. Horses were administered 100 mg/kg dextrose as a 20% solution (diluted in 0.9% saline) over 5 minutes. Blood was collected for glucose and insulin analysis at 6, 8, 10, 12, 15, 18, 20, 23, 26, 30, 40, 50, 60, 90, 120, 150 and 180 minutes. Ten mL of waste blood was collected from the sampling catheter, followed by 10 mL of blood which was divided between the fluoride oxalate (4 mL) and plain tubes (6 mL), and the catheter was then flushed with 20 mL of heparinized saline. Immediately following sample collection of the 20-minute time point, 20 mU/kg regular insulin was administered to each horse through the administration catheter. Blood glucose was measured in whole blood within 30 seconds of collection using a handheld glucometer³ validated for use in horses[70], according to the manufacturer's instructions. Blood collected into plain tubes was allowed to clot, and then centrifuged at 2500 rpm for 10 minutes. Plasma and serum were separated and stored at -80 C until analysis. Insulin concentration was measured on thawed serum samples using an equine insulin ELISA⁴. Minimal model analysis⁵ was used to calculate the insulin sensitivity (S_I) and insulin resistance index (I_R). Insulin resistant (IR) was defined as $S_I < 1.0 \times 10^{-4}$ L/mU/min from minimal model analysis[21, 69-71], and the clinically used cut-off of basal insulin >20 μ IU/mL[73, 74].

3.3 Echocardiography

Echocardiography was performed by an experienced operator using a portable ultrasonographic device⁶ equipped with a 1.5- to 4-MHz multifrequency sectorial transducer, with simultaneous ECG recording. All echocardiographic variables were measured using the mean of 3

² Extended Use MILACATH, MILA International Inc, Florence, Kentucky

³ AlphaTRAK 2 (code 5), Zoetis Inc, Kalamazoo, Michigan. Glucose strips: lot 1074309, exp 2020/12.

⁴ Mercodia Equine Insulin ELISA, Mercodia AB, Uppsala, Sweden. Kit lot #30096, exp 2022-02-28.

⁵ MINMOD Millenium 6.02, MinMod Inc

⁶ GE VIVID/I (BT12)

nonconsecutive cardiac cycles. Digitally stored recordings were used to perform all measurements offline, using electronic calipers embedded in the ultrasonographic device. Standard right and left parasternal views were used to obtain 2-D, M-mode, color Doppler images, and tissue Doppler images, enabling assessment of cardiac echogenicity, size, function, valvular competence and myocardial velocities. Two-dimensional variables included pulmonary artery diameter and aortic root diameter measured from right parasternal windows, and left atrial size measured from a standard left parasternal window. M-mode measurements were obtained from right parasternal short-axis views of the left ventricle at the level of the chordal attachments, and included left ventricular internal diameter during diastole and systole, interventricular septum thickness during diastole and systole, and left ventricular free wall thickness during diastole and systole. Previously reported equations[75] were used to calculate fractional shortening, MWT, RWT and LVM. TDI was used to obtain myocardial velocities and cardiac cycle intervals, and 2DST was used to calculate global circumferential strain.

3.4 *Non-invasive blood pressure measurements*

Blood pressure measurements were performed using an oscillometric monitor⁷ with the cuff centered over the coccygeal artery around the base of the unclipped tail. A bladder width-to-tail ratio of 0.4 to 0.6 was used in accordance with the instructions of the monitor manufacturer. Following discard of the first measurement obtained, three further measurements were then performed and recorded, and the mean calculated[76].

3.5 *Statistical analysis*

Microsoft Excel⁸ was used to generate descriptive statistics. Statistical software⁹ was used further analysis. Data were assessed for normality through fitting a normal distribution and performing a

⁷ Cardell Veterinary Monitor 9403, CAS Medical Systems, Branford, Connecticut.

⁸ Microsoft Excel for Mac, Version 16.16.6, 2018 Microsoft

⁹ JMP Pro 15 2.0, 2019 SAS Institute Inc

Goodness of Fit test (Shapiro-Wilk test). Pairwise Spearman correlation analysis was used for ordinal and non-normally distributed data. Pearson correlation analysis was used for normally distributed continuous data.

CHAPTER IV

RESULTS

4.1 *Horses*

Eleven horses were purchased from a sale barn. One horse was excluded due to the development of colic necessitating euthanasia, one horse was excluded due to temperament, two horses were excluded due to significant existing cardiac disease, one horse developed respiratory illness, and one horse was excluded due to pregnancy. Two horses were used from the OSU research herd. Summary of performed testing can be found in **Table 2**, and summary characteristics for the study population can be found in **Table 3**. The study sample consisted of 5 mares and 2 geldings, with a (mean \pm SD) weight of 524 ± 73 kg, body condition score 5.9 ± 1.2 , cresty neck score 2.4 ± 1.0 , and estimated age of 18 ± 4.2 years. Horse 1 was found to have a 2/6 systolic murmur with the PMI over the mitral valve. All nasal wash samples collected (horses 1-5) were negative for *S. equi* subsp. *equi* on qPCR, and hematology and serum biochemistry were unremarkable (see **Appendix 2**).

Table 2. Summary of testing performed, where ‘X’ denotes testing was performed on that horse, and (X) denotes testing was performed but data was excluded.

Horse	1	2	3	4	5	6	7
FSIGTT	X	(X)	X	X	(X)	X	X
Echo	X	X	X	X	X	X	X
NIBP	X	X	X	X	X		

FSIGTT, frequently sampled intravenous glucose tolerance test; *NIBP*, non-invasive blood pressure

4.2 FSIGTT

The sensitivity indices obtained from horses 2 and 5 were excluded from further analysis as the values obtained were considered to be physiologically impossible; this was presumed to be due to an error with sample handling. Results from the FSIGTT of each horse can be found in **Table 4**.

Table 3. Summary characteristics for study population.

Horse	1	2	3	4	5	6	7
Weight (kg)	433	547	592	610	488	562	434
Sex	G	M	M	M	G	M	M
BCS(9)[68]	4.5	6.0	5.0	6.0	5.0	7.0	8.0
CNS (5)[32]	2	1	2	3	2	3	4
Est. age (years)	23	15	17	12	23	15	19
Est. breed	Paint/pony	Paint	Paint	Paint	TB	Paint	Pony

CNS, Cresty Neck Score; *BCS*, body condition score; *TB*, Thoroughbred; *G*, gelding; *M*, mare

Horses were found to have a mean S_I of 2.21×10^{-4} L/min/mU, and median basal fasting insulin of 7.44 mU/L (IQR 5.51 – 18.43). Using a cut-off of $S_I < 1.0 \times 10^{-4}$ L/min/mU, horse 7 was classified as insulin resistant (IR)[21], whereas horses 4 and 7 were classified as IR using basal insulin concentration cut-off of > 9.7 mU/L.[25].

4.3 Echocardiography

Echocardiographic parameters may be found in **Table 5**. Horse 1 was found to have mild thickening of aortic valve (2+ jet, AR PHT 970 ms). Horse 2 was found to have misshapen pulmonic valve with mild pulmonic regurgitation. Horse 3 was found to have mild mitral regurgitation (3+), with two narrow but long jets. Horse 6 had a parallel fibrous band with 1+ aortic regurgitation. Horse 7 had an echoic area near the cranial papillary muscle, which was suspected to be a fibrous or fibrofatty infiltrate. Data for ET was missing for one horse (horse 6).

Table 4. Basal glucose and insulin concentrations, and results from minimal model analysis of FSIGTT.

		Horse						
Parameter	Units	1	2	3	4	5	6	7
G_b	mg/dL	109	118	117	124	94	114	120
I_b	mU/L	7.44	6.99	4.02	29.34	0.97	7.51	35.4
AIR_g	mU/L/min	188.22	68.71	231.05	475.86	73.32	187.58	436.66
DI		357.94	1644.10	1371.4	721.38	5884.20	316.75	14.26
DI FSD		0.24	29.05	0.02	0.71	47.38	0.04	2.6
S_I ($\times 10^{-4}$)	L/min/mU	1.90	23.93	5.94	1.516	5884.20	1.69	0.03
S_I FSD		0.24	29.05	0.02	0.71	47.38	0.04	2.6
S_G	min^{-1}		0.01	0.02	0.01	0.00	0.01	0.01
S_G FSD		0.04	0.05	0.04	0.13	351.57	0.07	0.15
GEZI	min^{-1}	0.01	0.00	0.03	0.00	0.00	0.01	0.01
GEZI FSD		0.04	2817.5	0.04	0.74	80.80	0.09	0.19
$HOMA_\beta$	μmM	59.52	51.36	22.97	190.31	12.93	51.50	174.58
$HOMA_{IR}$	$\text{mM}\cdot\text{mU}/\text{L}^2$	1.98	1.93	1.25	8.58	0.22	2.14	11.89
R^2	%	99.17	98.78	97.89	97.77	98.47	99.00	96.78

AIR_g , acute insulin response to glucose; DI , disposition index; FSD , fractional standard deviation; G_b , basal glucose; $GEZI$, glucose effectiveness at zero insulin; $HOMA_\beta$, β -cell function; $HOMA_{IR}$, insulin resistance; I_b , basal insulin; S_G , glucose effectiveness; S_I , insulin sensitivity.

Table 5. Echocardiographic measurements (n = 7). GSC data are presented as median (IQR1-IQR3). due to non-normal distribution

	Parameter	Mean \pm SD	Range	Units
2D	PAD	6.5 \pm 0.4	6.0 – 7.1	cm
	AoD	6.5 \pm 0.5	6.5 – 8.0	cm
	LADmax	10.7 \pm 0.5	9.8 – 11.3	cm
	LAAmax	81.5 \pm 9.4	67.1 – 91.4	cm^2
	LAAa	70.1 \pm 4.3	62.4 – 74.2	cm^2
	LAAmin	47.4 \pm 4.0	40.8 – 50.9	cm^2
	Ac LA FAC	32.3 \pm 5.5	26.2 – 43.3	%
	Pa LA FAC	13.1 \pm 9.8	0.1 – 25.5	%
	LA-RI _(area)	73.1 \pm 26.3	44.2 – 124.0	%
	LVIAd	126.7 \pm 12.7	103.6 – 142.8	cm^2
	LVIAs	54.0 \pm 6.2	43.1 – 63.0	cm^2
	SV	687 \pm 111	518 – 822	mL
	SV MOD	629 \pm 110	450 – 765	mL
	CO	28.14 \pm 8.85	17.34 – 43.16	L/min
	Co mod	25.77 \pm 8.30	15.08 – 40.18	L/min
	RR	1576 \pm 236	1135 – 1863	ms

	LADLmax	11.6 ± 0.8	10.6 – 12.5	cm
Mmode	LVIDs	6.1 ± 0.4	5.6 – 6.7	cm
	LVIDd	10.6 ± 0.6	9.5 – 11.4	cm
	IVSs	4.4 ± 0.2	3.9 – 4.6	cm
	IVSd	2.7 ± 0.2	2.4 – 3.0	cm
	FS	43 ± 4	37 – 48	%
	LVFWs	3.6 ± 0.4	2.9 – 4.0	cm
	LVFWd	2.0 ± 0.2	1.8 – 2.3	cm
	RWT	0.46 ± 0.03	0.40 – 0.48	
	MWT	2.40 ± 0.14	2.20 – 2.55	cm
	LVMass	2591 ± 366	1983 – 3009	g
	EPSS	4.1 ± 1.9	2 – 7	mm
	PEP	68 ± 19	42 – 101	ms
	ET	467 ± 31	274 – 501	ms
	RVIDd	3.1 ± 0.2	2.8 – 3.3	cm
	RVIDs	2.8 ± 0.7	2.1 – 4.2	cm
TDI	Variables of LV systolic function			
	S ₁	6.9 ± 1.3	5.0 – 9.0	cm/s
	S _m	11.0 ± 3.1	6.0 – 14.0	cm/s
	PEP _m	92 ± 7	31 – 101	ms
	IVCT _m	118.3 ± 25.4	85 – 161	ms
	ET _m	435 ± 28	392 – 471	ms
	Variables of LV diastolic function			
	E ₁	7.9 ± 0.6	7.0 – 9.0	cm/s
	E _m	22.9 ± 2.3	21.0 – 27.0	cm/s
	E _m /A _m	2.30 ± 0.45	1.50 – 3.00	
	IVRT _m	64.4 ± 17.7	42 – 87	ms
	Variables of active LA function			
	A _m	10.3 ± 2.2	7.0 – 14.0	cm/s
	LA velocity	8.4 ± 1.4	7.0 – 11.0	cm/s
	2DST	GSC	-16.5 (-17.1 – -15.0)	-17.5 – -12.9

4.4 Non-invasive blood pressure measurements

Horses had mean (± SD) systolic, diastolic and mean arterial blood pressures of 121 ± 13, 70 ± 17, and 87 ± 14 mm Hg, respectively (**Table 6**). NIBP was not performed in horses 6 and 7, and was unable to be collected from horse 5 due to poor temperament.

Table 6. Non-invasive blood pressure measurements (n = 4). All measurements were collected with a #10 cuff size. Values reported as systolic/diastolic (mean arterial) pressures.

	Horse			
	1	2	3	4
Blood pressure (mm Hg)	112/50 (71)	135/84 (97)	112/71 (85)	134/75 (97)
	112/48 (69)	129/86 (98)	104/65 (81)	131/79 (97)
	107/44 (67)	137/90 (108)	111/66 (85)	123/78 (94)
Average (mm Hg)	110/47 (69)	134/87 (101)	109/67 (84)	129/77 (96)
Reference[77] [†] (mm Hg)		Systolic 121 ± 11		
		Diastolic 72 ± 15		
		MAP 89 ± 13		

[†]Uncorrected for the height of the tail.

4.5 Statistical analyses

Non-normally distributed parameters included HOMA_{IR}, HOMA_β, DI, I_b, and GSC. These parameters and ordinal data were analyzed using Spearman correlation. Remaining variables were normally distributed and were analyzed using Pearson correlation. Parameters of insulin dysregulation (S_I, HOMA_β, HOMA_{IR}, etc) were compared pairwise with echocardiographic parameters of cardiac function (see Appendix). Using Pearson correlation analysis, S_I was positively correlated with peak velocity of the myocardium during the period of diastole corresponding with active atrial contraction (A_m, r = 0.89, p = 0.0419), and negatively correlated with isovolumetric relaxation time (IVRT_m, r = -0.97, p = 0.0072). Insulin sensitivity was also negatively correlated with ratio of myocardial velocities during early (E_m) and late diastole (A_m) (E_m/A_m, r = -0.92 p = 0.0263) (**Figures 5-7**).

A significant negative correlation was also found between S_I and CNS (p = 0.0138), and IVCT_m (p = 0.0374) using Spearman analysis (**Figures 8 and 9**).

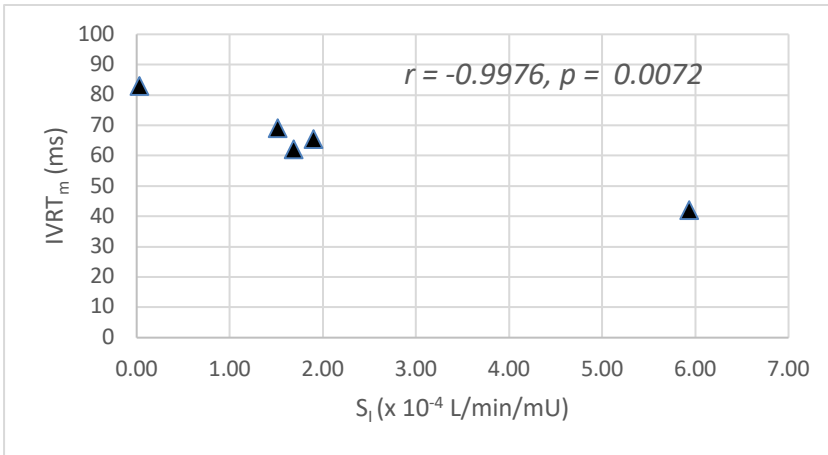


Figure 5. Correlation between isovolumetric relaxation time (IVRT_m) and insulin sensitivity (S_I).

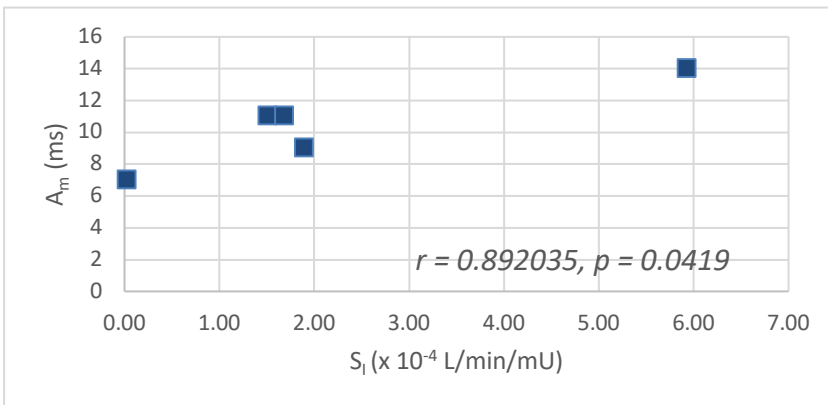


Figure 6. Correlation between peak myocardial velocity during active atrial contraction in late diastole (A_m), and insulin sensitivity (S_I).

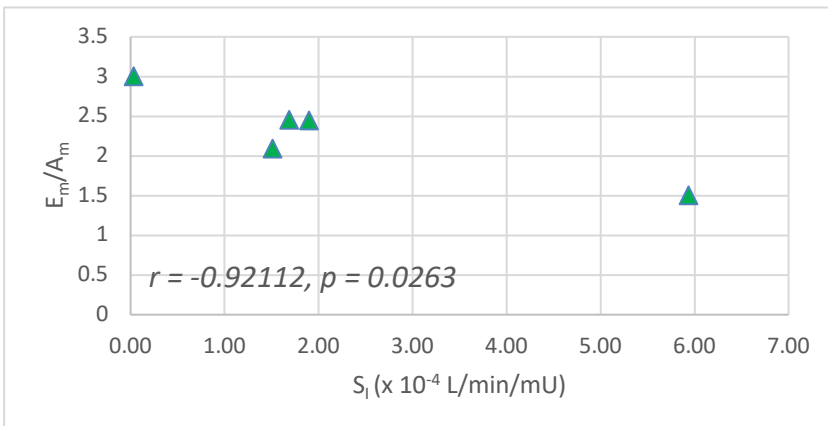


Figure 7. Correlation between ratio of myocardial velocity during early (E_m) and late (A_m) diastole, and insulin sensitivity (S_I).

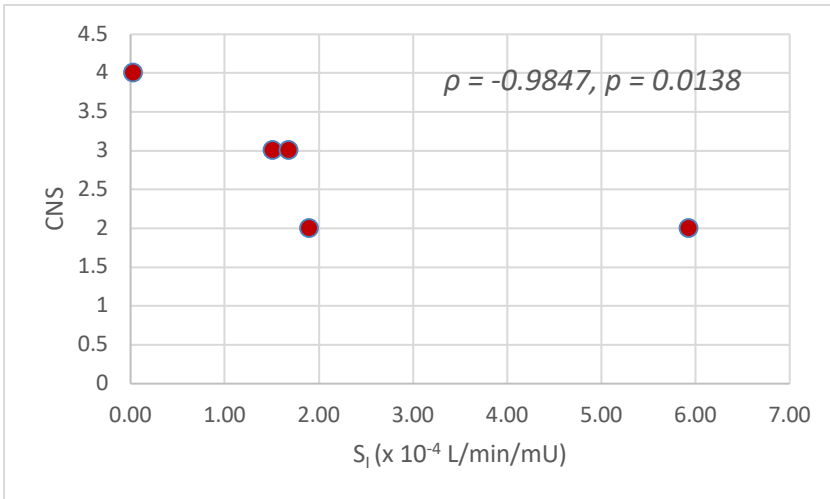


Figure 8. Correlation between cresty neck score (CNS) and insulin sensitivity (S_1).

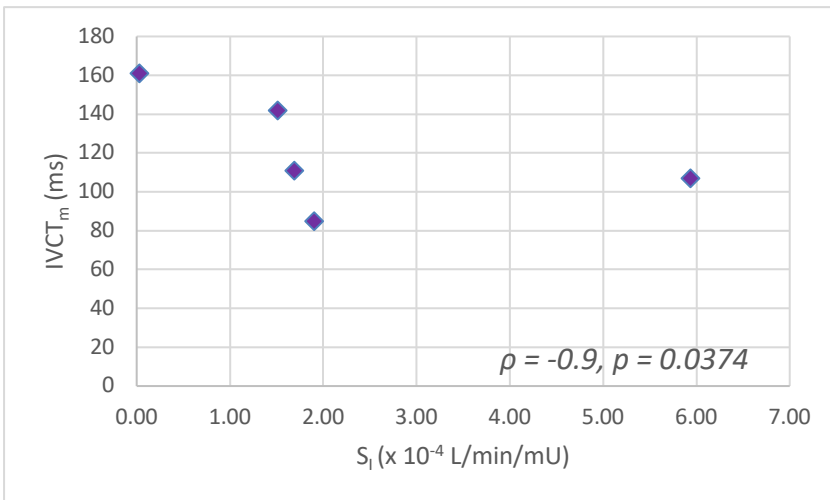


Figure 9. Correlation between isovolumetric contraction time (IVCT_m) and insulin sensitivity (S_1).

No significant correlations were found between insulin sensitivity and blood pressure, nor with measures of ventricular hypertrophy (Appendix).

CHAPTER V

CONCLUSION

5.1 *Insulin sensitivity*

The insulin sensitivity index (S_I) reflects insulin-dependent glucose clearance. In the current study, only 1 horse was classified as insulin resistant ($S_I = 0.03$ L/min/mU) using the cut-off of $S_I < 1.0 \times 10^{-4}$ L/min/mU proposed by Burns *et al* (2010)[21], with five horses classified as insulin sensitive (S_I ranges 1.515 to 5.94 L/min/mU), based on the proposed cut-off of $S_I < 1.0 \times 10^{-4}$ L/min/mU[21]. In the study by Burns *et al* (2010)[21], the authors performed minimal model analysis on data obtained from a FSIGTT. Notable differences exist between the methodology of that study and the study reported here, including differences in their FSIGTT protocol (500 mg/kg dextrose IV) and insulin dosage and measurement (100 mU/kg, radioimmunoassay). Due to the various methods for measuring insulin[76-80] and variations on FSGITT protocols[16, 22, 67], comparing results between studies presents a challenge. The intention of the study reported here was to obtain quantitative measurements of degree of insulin sensitivity in order to compare with various cardiac parameters, and this goal was achieved.

Using a fasting insulin cut-off of >9.5 of $\mu\text{IU/mL}$ [25], two horses in this study (horses 5 and 7) would have been classified as insulin resistant. Compared with the gold standard of EHC, fasting insulin, as measured with the Mercodia equine insulin ELISA, has been reported to have a

sensitivity and specificity of 91% and 85%, respectively, for diagnosing insulin resistance using the cut-off of >9.5 of $\mu\text{IU/mL}$ [25]. Many different cut-offs have been described for categorizing horses as insulin resistant, and it is important to note that cut-offs vary depending on the laboratory and assay used for measurement of insulin. The utility of using fasting insulin for the diagnosis of insulin resistance continues to be debated, as fasting alone may put horses into an insulin-resistant state[14].

Two of the sensitivity indices in this study were unrealistically high and excluded from further analysis (horses 2 and 5). Horse 5 had very low basal insulin concentrations, and since this horse had normal basal glucose concentrations (*ie* not hyperglycemic), it is unlikely that this horse had true hypoinsulinemia. The etiology of the high S_1 of horse 2 was not apparent from the glucose and insulin curves.

5.2 *Myocardial function*

Our study found significant correlations between insulin sensitivity and indices of both diastolic and systolic function. To the author's knowledge, this is the first study to investigate the relationship between insulin sensitivity and its effect on myocardial function as evaluated with TDI and 2DST. Comparing systolic and diastolic functional indices between humans and horses is challenging due to the associated difficulties in reliably obtaining certain echocardiographic measurements in horses. In humans, Doppler-derived transmitral flow velocities (E wave, A wave, E/A ratio, E-wave deceleration time, and deceleration slope) are commonly used in combination with TDI-derived wall motion velocities (E_m , A_m , E_m/A_m ratio) for the assessment of diastolic LV and filling pressures[42]. Decreased E/A ratio[63, 81-83], increased A velocity[35, 63, 83], and decreased E velocity[63], have all been found in humans with MetS. In adult horses however, PW Doppler recordings of transmitral flow velocities are difficult to obtain and relatively unreliable[41, 50].

5.2.1 *Systolic function*

Decreases in insulin sensitivity were associated with increases in isovolumetric contraction time (IVCT_m, $\rho = -0.94$, $p = 0.04$), suggesting impaired systolic contractile function. Isovolumetric contraction time represents the time period in early systole following closure of the atrioventricular valves, but before enough intraventricular pressure has been generated to open the semilunar valves. Systolic dysfunction has also been documented in humans with MetS, as evidenced by decreases in ϵ , strain rate and S_m [35, 62, 63]. Although IVCT_m has been found to be significantly increased in horses with moderate to severe mitral valve regurgitation (MR)[43], only one horse in the present study had MR, and regurgitation was considered to be mild.

A decrease in preload can also increase pre-ejection period and decrease LV ejection time, causing decreases in systolic time intervals[43]. Decreases in preload may be reflected by decreases in LADmax, LA Amax and LVIDd[43]. Higher heart rates also result in decreased preload, as higher heart rates result in shorter filling times for both the LA and LV[43]. None of the horses in this study had increased heart rates, and no correlations were found between parameters of preload and systolic time intervals, thus the observed systolic time intervals are unlikely to have been affected by preload.

Our study did not find a correlation between insulin sensitivity and global circumferential strain (ϵ). When strain is used as index of systolic function, shortening is indicated by negative strain. Thus, the more negative the strain, the better the LV systolic function. In humans, MetS is significantly associated with less circumferential myocardial shortening as indicated by less negative LV circumferential strain (ϵ_{CC})[64], and less longitudinal myocardial shortening as indicated by less negative LV longitudinal strain (ϵ_{LL})[64]. The magnitude of changes in mean systolic strain and peak systolic strain rate also increased with number of components of MetS[35, 63]. Other measures of systolic function found to be significantly decreased in humans

with MetS include TDI-derived systolic septal myocardial velocity (a measure of longitudinal myocardial contractility)[85], and peak myocardial systolic velocity (S_m)[35, 83]. The lack of association found between insulin sensitivity and cardiac strain or peak systolic myocardial velocity in our study may represent species differences in cardiac metabolism. However, it is also important to note our study was comprised of a very small sample size, and only one horse was classified as insulin resistant, thus further studies with larger numbers of both insulin-sensitive and insulin-resistant horses are needed to investigate this relationship.

5.2.2 *Diastolic function*

In our study, insulin sensitivity was negatively correlated with diastolic dysfunction, as evidenced by a decrease in myocardial velocity associated with active atrial contraction (A_m , $r = 0.89$, $p = 0.04$), and an increase in isovolumetric relaxation time ($IVRT_m$, $r = -0.9976$, $p = 0.0072$) with decreases in S_l . Isovolumetric relaxation time represents the time from the end of systole following closure of the semilunar valves and prior to opening of the atrioventricular valves, and is a sensitive measure of diastolic function. An increase in this time is reflective of a delay in myocardial relaxation, and that more time is required for enough pressure change to occur within the ventricle to induce opening of the mitral valve. Delays in myocardial relaxation may occur with catecholamine stimulation induced increases in afterload, and with aging-associated fibrosis of the ventricle[42]. Tachycardia may also decrease the time available for myocardial relaxation. MetS in humans has been associated with an increase in $IVRT_m$ [85], in addition to decreased peak early diastolic SR[35, 63].

This study found E_m/A_m ratio increased as insulin sensitivity decreased, in contrast to the decreased E_m/A_m ratio as has been found in humans with MetS[84]. The current study found a significant negative correlation between insulin sensitivity and peak radial wall motion velocity in late diastole (A_m), suggesting atrial dysfunction. In humans, MetS is associated with early

diastolic dysfunction, as evidenced by reduced peak radial wall motion velocity in early diastole (E_m)[35, 83, 84], with resultant decrease in the E_m/A_m ratio[84]. TDI-derived early diastolic myocardial velocities were significantly lower in both MetS and pre-MetS humans than in controls, suggesting progressive impairment in LV relaxation as the number of MetS criteria increase[85]. This difference may represent species differences with respect to the metabolism of the atrial myocardium in the presence of insulin dysregulation, and requires further investigation.

A marked decrease in E_m and E_m/A_m ratio has been postulated to represent a hallmark of LV diastolic dysfunction in horses with myocardial disease[43]. In a previous study by Koenig *et al*, horses with myocardial disease showed a marked decrease in E_m with a nonsignificant increase in A_m velocity and a resulting significant decrease in E_m/A_m ratio[43], suggesting impaired ventricular relaxation with a compensatory increase in left atrial booster pump function in an attempt to maintain cardiac output[43]. These findings are in contrast to the current study (decreased A_m and increased E_m/A_m ratio), and it is important to note that the horses in the Koenig *et al* study had significant myocardial disease. It is likely that different areas of the myocardium are affected by insulin dysregulation, and it is difficult to make comparisons as the etiology of myocardial disease in the aforementioned study was not given.

In humans, myocardial systolic and diastolic function have been found to decrease with age, leading to decreased S_m and E_m , and increased A_m velocities[39]. In a population of healthy warmblood horses, age was not found to significantly influence PW TDI variables [43], however the mean age in that study was 12 ± 4 years. The mean age of horses in the current study was older at 17 ± 4 years, and this may have confounded the differences in myocardial velocities. The influence of age on E_m , A_m and other TDI variables requires further investigation.

5.3 *Myocardial hypertrophy*

In this study, there was no significant correlation of S_I with relative wall thickness (RWT), mean wall thickness (MWT) or LV mass, which are indices reflective of ventricular remodeling. This is in contrast to another study (Heliczzer *et al*) which found ponies with EMS had increased MWT and RWT without increases in LV mass[8], indicative of concentric remodeling. In humans, MetS is associated with increased RWT[83, 84], indicating concentric remodeling. An increased LV mass has also been reported in humans with MetS[62, 84], however this finding was found to be more strongly associated with blood pressure[84]. The study by Heliczzer *et al* found that MWT and RWT were increased in Shetland ponies with EMS compared to controls, however for all ponies, only RWT was increased in the cases with EMS, which may imply an existence of breed differences in response to metabolic syndrome. Duration of insulin resistance may also be an important factor in the development of gross cardiac remodeling, which requires further investigation.

In our study, insulin sensitivity was not correlated with blood pressure. Studies in ponies have reported hypertension associated with metabolic syndrome[7, 8]. The study by Heliczzer *et al* (2017)[8] found that in Shetland ponies, but not all ponies, those with EMS had significant increases in systolic and mean arterial blood pressures compared to controls. It is important to note that in the study by Heliczzer *et al*, cases were designated as having EMS based on history of laminitis, body condition score ($\geq 7/9$), cresty neck score ($\geq 3/5$), and abnormal oral sugar test results (using a dosage of 0.15 mL/kg corn syrup). As the oral sugar test lacks sensitivity, but is very specific, for the diagnosis of insulin resistance[73], the ponies used in the aforementioned study are likely to have had much greater degrees of insulin resistance compared to the horses in our study population, which may account for differences seen.

5.4 *Other findings*

Correlation was found between cresty neck score (CNS) and insulin sensitivity index ($\rho = -0.95$, $p = 0.0138$). In a previous study, CNS was found to moderately correlate with insulin, glucose and triglyceride concentrations in both horses and ponies[32]. However, to the author's knowledge, direct correlation between CNS and S_I *per se* has not been yet reported.

5.5 *Limitations*

This study had several limitations, including a very small sample size, and inconsistent testing performed for each horse; the study was thus limited by low power. For instance, to detect a relevant simple correlation (eg $r = 0.4$) for 6 observations (eg $ICVT_m$, $IVRT_m$, E_m , E_m/A_m ratio, S_m , and ϵ), with significance of $\alpha = 0.05$ and power ($1 - \beta$) of 0.8, the required sample size would be $n = 10$.

Only one of the horses in our study met the criteria for EMS (horse 7), which limited our ability to investigate the relationship between cardiac function and more marked degrees of insulin resistance. Testing for pars pituitary intermedia dysfunction (PPID) was not performed in our study, which impedes making a distinction between insulin dysregulation (ID) associated with metabolic syndrome, or that associated with PPID in our study population. Both EMS and PPID are associated with an increased risk of developing laminitis, which is likely related to ID[6]. EMS and PPID can coexist, and a subset of animals with PPID have ID[6]. Aged horses (>15 years) have increased odds (OR 1.2) of having PPID[87], with the risk increasing with increasing age[87]. This is of particular relevance to the current study population, as the youngest horse was estimated to be approximately 12-years-old, and 5/7 horses were known or estimated to be ≥ 15 -years-old. Although ID may exist in both EMS and PPID, the overlap between mechanisms of ID, such as β -cell dysfunction or tissue insulin resistance, is unknown.

Many aspects of the study were not blinded, and the same investigator performing cresty neck and body condition scores (NW) was not blinded to blood glucose and serum insulin curves. It is unlikely that the lack of blinding in this study would have influenced outcomes.

Echocardiographic measurements were only performed once, which may have resulted in some variability in measurements going undetected. Another limitation was that inherent to the Doppler technique itself, as velocities are measured relative to the transducer, in the direction of the ultrasonographic beam. Velocity measurements are thus affected by total heart motion and by the insonation angle between the ultrasonographic beam and wall motion.

5.6 *Conclusion*

This study found insulin sensitivity correlated with cardiac dysfunction in horses. In both humans with metabolic disease and horses with documented cardiac disease, the use of myocardial tissue velocities has enabled the detection of existing myocardial dysfunction prior to the occurrence of changes in more traditional measures of cardiac dysfunction. Insulin resistance was found to negatively impact both systolic and diastolic function. As opposed to the impaired ventricular myocardial relaxation seen in humans with insulin resistance, diastolic dysfunction in horses with insulin resistance was compounded by atrial dysfunction. The reasons for the negative impact of insulin resistance on systolic function were not apparent, and further investigation using larger sample sizes will likely provide more insight into this relationship. The results of this study must be interpreted with caution due to the small sample size, and the relationship between insulin sensitivity and subclinical ventricular dysfunction in horses requires further investigation. Future work includes larger sample sizes, and investigating the relationship between insulin sensitivity index and vulnerability of induction to AF, and heart rate variability, a measure of sympathetic tone.

REFERENCES

1. *Executive Summary of The Third Report of The National Cholesterol Education Program (NCEP) Expert Panel on Detection, Evaluation, And Treatment of High Blood Cholesterol In Adults (Adult Treatment Panel III)*. *Jama*, 2001. **285**(19): p. 2486-97.
2. Ford ES, G.W., *A comparison of the prevalence of the metabolic syndrome using two proposed definitions*. *Diabetes Care*, 2003. **26**(3): p. 575-581.
3. Isomaa, B., et al., *Cardiovascular morbidity and mortality associated with the metabolic syndrome*. *Diabetes Care*, 2001. **24**(4): p. 683-9.
4. Mazumder, P.K., et al., *Impaired cardiac efficiency and increased fatty acid oxidation in insulin-resistant ob/ob mouse hearts*. *Diabetes*, 2004. **53**(9): p. 2366-74.
5. Gami, A.S., et al., *Metabolic syndrome and risk of incident cardiovascular events and death: a systematic review and meta-analysis of longitudinal studies*. *J Am Coll Cardiol*, 2007. **49**(4): p. 403-14.
6. Durham, A.E., et al., *ECEIM consensus statement on equine metabolic syndrome*. *J Vet Intern Med*, 2019. **33**(2): p. 335-349.
7. Bailey SR, H.-B.J., Ransom KJ, Elliott J, Menzies-Gow NJ. , *Hypertension and insulin resistance in a mixed-breed population of ponies predisposed to laminitis*. *American Journal of Veterinary Research.*, 2008. **69**(1): p. 122-129.
8. Heliczner N, G.V., Bruckmaier R, van der Kolk JH, Navas de Solis C, *Cardiovascular findings in ponies with equine metabolic syndrome*. *Journal of the American Veterinary Medical Association*, 2017. **250**(9): p. 1027-1035.
9. Cefalu, W.T., *Insulin resistance: cellular and clinical concepts*. *Experimental biology and medicine*, 2001. **226**(1): p. 13-26.
10. Reaven, G., *The metabolic syndrome or the insulin resistance syndrome? Different names, different concepts, and different goals*. *Endocrinol Metab Clin North Am*, 2004. **33**(2): p. 283-303.
11. Kronfeld, D.S., K.H. Treiber, and R.J. Geor, *Comparison of nonspecific indications and quantitative methods for the assessment of insulin resistance in horses and ponies*. *Journal of the American Veterinary Medical Association*, 2005. **226**(5): p. 712-719.
12. Bergman, R.N., L.S. Phillips, and C. Cobelli, *Physiologic evaluation of factors controlling glucose tolerance in man: measurement of insulin sensitivity and beta-cell glucose sensitivity from the response to intravenous glucose*. *The Journal of clinical investigation*, 1981. **68**(6): p. 1456-1467.
13. Wallace, T. and D. Matthews, *The assessment of insulin resistance in man*. *Diabetic medicine*, 2002. **19**(7): p. 527-534.
14. Bertin, F.-R. and M. De Laat, *The diagnosis of equine insulin dysregulation*. *Equine veterinary journal*, 2017. **49**(5): p. 570-576.
15. Muniyappa, R., et al., *Current approaches for assessing insulin sensitivity and resistance in vivo: advantages, limitations, and appropriate usage*. *American Journal of Physiology-Endocrinology and Metabolism*, 2008. **294**(1): p. E15-E26.

16. Pratt, S.E., R.J. Geor, and L.J. McCutcheon, *Repeatability of 2 methods for assessment of insulin sensitivity and glucose dynamics in horses*. J Vet Intern Med, 2005. **19**(6): p. 883-8.
17. Bergman, R.N., et al., *Equivalence of the insulin sensitivity index in man derived by the minimal model method and the euglycemic glucose clamp*. J Clin Invest, 1987. **79**(3): p. 790-800.
18. Wilcox, G., *Insulin and insulin resistance*. Clin Biochem Rev, 2005. **26**(2): p. 19-39.
19. Bailey, S.R., et al., *Effect of dietary fructans and dexamethasone administration on the insulin response of ponies predisposed to laminitis*. Journal of the American Veterinary Medical Association, 2007. **231**(9): p. 1365-1373.
20. Hoffman, R., et al., *Obesity and diet affect glucose dynamics and insulin sensitivity in Thoroughbred geldings*. Journal of animal science, 2003. **81**(9): p. 2333-2342.
21. Burns, T.A., et al., *Proinflammatory cytokine and chemokine gene expression profiles in subcutaneous and visceral adipose tissue depots of insulin-resistant and insulin-sensitive light breed horses*. J Vet Intern Med, 2010. **24**(4): p. 932-9.
22. Pratt-Phillips, S.E., R.J. Geor, and L.J. McCutcheon, *Comparison among the euglycemic-hyperinsulinemic clamp, insulin-modified frequently sampled intravenous glucose tolerance test, and oral glucose tolerance test for assessment of insulin sensitivity in healthy Standardbreds*. Am J Vet Res, 2015. **76**(1): p. 84-91.
23. Boston, R.C., et al., *MINMOD Millennium: a computer program to calculate glucose effectiveness and insulin sensitivity from the frequently sampled intravenous glucose tolerance test*. Diabetes Technol Ther, 2003. **5**(6): p. 1003-15.
24. Matthews DR, H.J., Rudenski AS, Naylor BA, Treacher DF, Turner RC. , *Homeostasis model assessment: insulin resistance and beta-cell function from fasting plasma glucose and insulin concentrations in man*. Diabetologia, 1985. **28**: p. 412-419.
25. Truelsen Lindåse, S., et al., *Evaluation of fasting plasma insulin and proxy measurements to assess insulin sensitivity in horses*. 2021.
26. Olley, R., et al., *Comparison of fasted basal insulin with the combined glucose-insulin test in horses and ponies with suspected insulin dysregulation*. The Veterinary Journal, 2019. **252**: p. 105351.
27. Cheng, Y.-H., et al., *Body mass index and waist circumference are better predictors of insulin resistance than total body fat percentage in middle-aged and elderly Taiwanese*. Medicine, 2017. **96**(39).
28. Treiber KH, K.D., Hess TM, Byrd BM, Splan RK, Staniar WB. , *Evaluation of genetic and metabolic predispositions and nutritional risk factors for pasture-associated laminitis in ponies*. Journal of the American Veterinary Medical Association, 2006. **228**: p. 1538-1545.
29. Johnson, P.J., *The equine metabolic syndrome: Peripheral Cushing's syndrome*. Veterinary Clinics: Equine Practice, 2002. **18**(2): p. 271-293.
30. Carter RA, G.R., Staniar WB, Cubitt TA, Harris PA, *Apparent adiposity assessed by standardised scoring systems and morphometric measurements in horses and ponies*. The Veterinary Journal, 2008. **179**: p. 204-210.
31. Giles, S.L., et al., *Assessing the seasonal prevalence and risk factors for nuchal crest adiposity in domestic horses and ponies using the Cresty Neck Score*. BMC Veterinary Research, 2015. **11**(1): p. 13.
32. Fitzgerald, D.M., et al., *The cresty neck score is an independent predictor of insulin dysregulation in ponies*. Plos one, 2019. **14**(7): p. e0220203.
33. Schwarzwald, C.C., *Ultrasonography of the equine heart*, in *Atlas of Equine Ultrasonography*, J.A.L. Kidd, K.G.; Frazer, M.L., Editor. 2014, John Wiley & Sons, Ltd.: West Sussex, UK. p. 379-406.

34. Støylen, A. *Strain rate imaging*. 2016 October 2020 [cited 2020 13/1].
35. Wong, C.Y., et al., *Myocardial and vascular dysfunction and exercise capacity in the metabolic syndrome*. *Am J Cardiol*, 2005. **96**(12): p. 1686-91.
36. Dandel, M., et al., *Strain and strain rate imaging by echocardiography - basic concepts and clinical applicability*. *Curr Cardiol Rev*, 2009. **5**(2): p. 133-48.
37. Johnson, C., et al., *Practical tips and tricks in measuring strain, strain rate and twist for the left and right ventricles*. *Echo research and practice*, 2019. **6**(3): p. R87-R98.
38. Schwarzwald, C.C., *Equine echocardiography*. *Veterinary Clinics: Equine Practice*, 2019. **35**(1): p. 43-64.
39. Kadappu, K.K. and L. Thomas, *Tissue Doppler imaging in echocardiography: value and limitations*. *Heart Lung Circ*, 2015. **24**(3): p. 224-33.
40. Nagueh, S.F., et al., *Recommendations for the evaluation of left ventricular diastolic function by echocardiography: an update from the American Society of Echocardiography and the European Association of Cardiovascular Imaging*. *European Journal of Echocardiography*, 2016. **17**(12): p. 1321-1360.
41. Koenig, T.R., K.J. Mitchell, and C.C. Schwarzwald, *Echocardiographic Assessment of Left Ventricular Function in Healthy Horses and in Horses with Heart Disease Using Pulsed-Wave Tissue Doppler Imaging*. *J Vet Intern Med*, 2017. **31**(2): p. 556-567.
42. Decloedt, A., et al., *Evaluation of tissue Doppler imaging for regional quantification of radial left ventricular wall motion in healthy horses*. *Am J Vet Res*, 2013. **74**(1): p. 53-61.
43. Schwarzwald, C.C., K. Schober, and J. Bonagura, *Methods and reliability of tissue Doppler imaging for assessment of left ventricular radial wall motion in horses*. *Journal of veterinary internal medicine*, 2009. **23**(3): p. 643-652.
44. LONG, K.J., J. Bonagura, and P. Darke, *Standardised imaging technique for guided M-mode and Doppler echocardiography in the horse*. *Equine veterinary journal*, 1992. **24**(3): p. 226-235.
45. Patteson, M., et al., *Echocardiographic measurements of cardiac dimensions and indices of cardiac function in normal adult thoroughbred horses*. *Equine Veterinary Journal*, 1995. **27**(S19): p. 18-27.
46. Decloedt, A., et al., *Tissue Doppler Imaging and 2-Dimensional Speckle Tracking of Left Ventricular Function in Horses Exposed to Lasalocid*. *Journal of Veterinary Internal Medicine*, 2012. **26**(5): p. 1209-1216.
47. Schefer, K., et al., *Laboratory, electrocardiographic, and echocardiographic detection of myocardial damage and dysfunction in an Arabian mare with nutritional masseter myodegeneration*. *Journal of veterinary internal medicine*, 2011. **25**(5): p. 1171-1180.
48. Schwarzwald, C.C., K.E. Schober, and J.D. Bonagura, *Methods and reliability of echocardiographic assessment of left atrial size and mechanical function in horses*. *American journal of veterinary research*, 2007. **68**(7): p. 735-747.
49. Schwarzwald, C.C., K.E. Schober, and J.D. Bonagura, *Echocardiographic evidence of left atrial mechanical dysfunction after conversion of atrial fibrillation to sinus rhythm in 5 horses*. *Journal of veterinary internal medicine*, 2007. **21**(4): p. 820-827.
50. Blissitt, K.J. and J. Bonagura, *Pulsed wave Doppler echocardiography in normal horses*. *Equine veterinary journal*, 1995. **27**(S19): p. 38-46.
51. Schefer, K.D., et al., *Quantitative analysis of stress echocardiograms in healthy horses with 2-dimensional (2D) echocardiography, anatomical M-mode, tissue Doppler imaging, and 2D speckle tracking*. *Journal of Veterinary Internal Medicine*, 2010. **24**(4): p. 918-931.
52. Verheyen, T., et al., *Cardiac Changes in Horses with Atypical Myopathy*. *Journal of Veterinary Internal Medicine*, 2012. **26**(4): p. 1019-1026.

53. Lang, R.M., et al., *Recommendations for cardiac chamber quantification by echocardiography in adults: an update from the American Society of Echocardiography and the European Association of Cardiovascular Imaging*. J Am Soc Echocardiogr, 2015. **28**(1): p. 1-39.e14.
54. De Clercq, D., et al., *Atrial and ventricular electrical and contractile remodeling and reverse remodeling owing to short-term pacing-induced atrial fibrillation in horses*. J Vet Intern Med, 2008. **22**(6): p. 1353-9.
55. Decloedt, A., et al., *Risk Factors for Recurrence of Atrial Fibrillation in Horses After Cardioversion to Sinus Rhythm*. Journal of Veterinary Internal Medicine, 2015. **29**(3): p. 946-953.
56. Decloedt, A., et al., *Echocardiographic measurements of right heart size and function in healthy horses*. Equine Veterinary Journal, 2017. **49**(1): p. 58-64.
57. Schwarzwald, C.C., et al., *Left Ventricular Radial and Circumferential Wall Motion Analysis in Horses Using Strain, Strain Rate, and Displacement by 2D Speckle Tracking*. Journal of Veterinary Internal Medicine, 2009. **23**(4): p. 890-900.
58. Decloedt, A., et al., *Quantification of Left Ventricular Longitudinal Strain, Strain Rate, Velocity, and Displacement in Healthy Horses by 2-Dimensional Speckle Tracking*. Journal of Veterinary Internal Medicine, 2011. **25**(2): p. 330-338.
59. DECLOEDT, A., et al., *Two-dimensional speckle tracking for quantification of left ventricular circumferential and radial wall motion in horses*. Equine Veterinary Journal, 2013. **45**(1): p. 47-55.
60. Mottillo, S., et al., *The metabolic syndrome and cardiovascular risk a systematic review and meta-analysis*. J Am Coll Cardiol, 2010. **56**(14): p. 1113-32.
61. Alberti KGMM, E.R., Grundy SM, Zimmet PZ, Cleeman JI, Donato KA, Fruchart J-C, James WPT, Loria CM, Smith SC JR, *Harmonizing the metabolic syndrome: a joint interim statement of the International Diabetes Federation Task Force on Epidemiology and Prevention; National Heart, Lung, and Blood Institute; American Heart Association; World Heart Federation; International Atherosclerosis Society; and International Association for the Study of Obesity*. Circulation, 2009. **120**: p. 1640-1645.
62. Almeida, A.L.C.d., et al., *Metabolic Syndrome, Strain, and Reduced Myocardial Function: Multi-Ethnic Study of Atherosclerosis*. Arquivos Brasileiros de Cardiologia, 2014. **102**(4): p. 327-335.
63. Gong, H.P., et al., *Impaired left ventricular systolic and diastolic function in patients with metabolic syndrome as assessed by strain and strain rate imaging*. Diabetes Res Clin Pract, 2009. **83**(3): p. 300-7.
64. Chang C-J, Y.Y.-C., Lu F-H, Lin T-S, Chen J-J, Yeh T-L, Wu C-H, Wu J-S. , *Altered cardiac autonomic function may precede insulin resistance in metabolic syndrome*. The American Journal of Medicine, 2010. **123**: p. 432-438.
65. Zibadi, S., et al., *Myocardial lysyl oxidase regulation of cardiac remodeling in a murine model of diet-induced metabolic syndrome*. Am J Physiol Heart Circ Physiol, 2009. **297**(3): p. H976-82.
66. Henneke DR, P.G., Kreider JL, Yeates BF, *Relationship between condition score, physical measurements and body fat percentage in mares*. Equine Veterinary Journal, 1983. **14**(4): p. 371-372.
67. Tóth F, F.N., Elliott SB, Perdue K, Geor RJ, Boston RC, *Optimisation of the frequently sampled intravenous glucose tolerance test to reduce urinary glucose spilling in horses*. Equine Veterinary Journal, 2009. **41**(9): p. 844-851.
68. Hackett ES, M.P., *Evaluation of a veterinary glucometer for use in horses*. Journal of Veterinary Internal Medicine, 2010. **24**: p. 617-621.

69. Toth, F., et al., *Measurement of C-peptide concentrations and responses to somatostatin, glucose infusion, and insulin resistance in horses*. Equine veterinary journal, 2010. **42**(2): p. 149-155.
70. Carter, R.A., et al., *Effects of exercise training on adiposity, insulin sensitivity, and plasma hormone and lipid concentrations in overweight or obese, insulin-resistant horses*. American journal of veterinary research, 2010. **71**(3): p. 314-321.
71. Dunbar, L., et al., *Evaluation of four diagnostic tests for insulin dysregulation in adult light-breed horses*. Journal of veterinary internal medicine, 2016. **30**(3): p. 885-891.
72. Frank, N., et al., *Equine metabolic syndrome*. Journal of veterinary internal medicine, 2010. **24**(3): p. 467-475.
73. Navas de Solis C, S.J., Boston RC, Reef VB. , *Hypertensive cardiomyopathy in horses: 5 cases (1995-2011)*. Journal of the American Veterinary Medical Association, 2013. **243**(1): p. 126-130.
74. Brown S, A.C., Bagley R, Carr A, Cowgill M, Davidson M, Egner B, Elliot J, Henik R, Labato M, Littman M, Polzin D, Ross L, Snyder P, Stepien R. , *Guidelines for the identification, evaluation, and management of systemic hypertension in dogs and cats*. Journal of Veterinary Internal Medicine, 2007. **21**(3): p. 542-558.
75. Parry BW, M.M., Anderson GA. , *Survey of resting blood pressure values in clinically normal horses*. Equine Veterinary Journal, 1984. **16**(1): p. 53-58.
76. Tinworth, K.D., et al., *Evaluation of commercially available assays for the measurement of equine insulin*. Domest Anim Endocrinol, 2011. **41**(2): p. 81-90.
77. Carslake, H.B., G.L. Pinchbeck, and C.M. McGowan, *Evaluation of a Chemiluminescent Immunoassay for Measurement of Equine Insulin*. J Vet Intern Med, 2017. **31**(2): p. 568-574.
78. Warnken, T., K. Huber, and K. Feige, *Comparison of three different methods for the quantification of equine insulin*. BMC Vet Res, 2016. **12**(1): p. 196.
79. Banse, H.E., et al., *Comparison of two methods for measurement of equine insulin*. J Vet Diagn Invest, 2014. **26**(4): p. 527-530.
80. Borer-Weir, K.E., et al., *Evaluation of a commercially available radioimmunoassay and species-specific ELISAs for measurement of high concentrations of insulin in equine serum*. Am J Vet Res, 2012. **73**(10): p. 1596-602.
81. Chinali, M., et al., *Comparison of cardiac structure and function in American Indians with and without the metabolic syndrome (the Strong Heart Study)*. Am J Cardiol, 2004. **93**(1): p. 40-4.
82. Fontes-Carvalho, R., et al., *Diastolic dysfunction in the diabetic continuum: association with insulin resistance, metabolic syndrome and type 2 diabetes*. Cardiovascular diabetology, 2015. **14**(1): p. 1-9.
83. Fuentes, L.d.l., et al., *Metabolic syndrome is associated with abnormal left ventricular diastolic function independent of left ventricular mass*. European heart journal, 2007. **28**(5): p. 553-559.
84. Grandi, A.M., et al., *Metabolic syndrome and morphofunctional characteristics of the left ventricle in clinically hypertensive nondiabetic subjects*. Am J Hypertens, 2006. **19**(2): p. 199-205.
85. McGowan, T., G. Pinchbeck, and C. McGowan, *Prevalence, risk factors and clinical signs predictive for equine pituitary pars intermedia dysfunction in aged horses*. Equine veterinary journal, 2013. **45**(1): p. 74-79.

APPENDICES

Table 7. Raw echocardiographic data for study horses. For parameters, see abbreviations list.

	HORSE	units	1	2	3	4	5	6	7	MEAN	SD	MEDIAN	IQR	MIN	MAX	
	ALIAS		#330	#331	#337	#348	#349	Hazel	Coco							
Weight (kg)	initial		433	547	592	610	488	562	434	523.7						
	PAD	cm	6.7	7.1	6.2	6.2	6.8	6.5	6	6.5	0.391578			6	7.1	
2d	AoD	cm	7.5	7.9	8	6.9	7.6	7.1	6.5	7.35714286	0.54728768			6.5	8	
	LADmax	cm	10.6	10.3	11.1	11.3	10.7	11	9.8	10.6857143	0.5145502			9.8	11.3	
	LAAmax	cm^2	75.6	87.4	73.4	89.9	85.5	91.4	67.1	81.4714286	9.37331572			67.1	91.4	
	LAAa	cm^2	73.3	74.2	73.3	67	68.7	71.9	62.4	70.1142857	4.30868447			62.4	74.2	
	LAAmin	cm^2	47.6	50.6	50.9	47.9	50.7	40.8	43.1	47.3714286	3.99404318			40.8	50.9	
	Ac LA FAC	%	35.0613915	31.8059299	30.5593452	28.5074627	26.2008734	43.2545202	30.9294872	32.3312871	5.54308756			26.2008734	43.2545202	
	Pa LA FAC	%	3.04232804	15.1029748	0.13623978	25.4727475	19.6491228	21.3347921	7.00447094	13.1060966	9.78238773			0.13623978	25.4727475	
	A Reservoir	%	58.8235294	72.7272727	44.2043222	87.6826722	68.6390533	124.019608	55.6844548	73.1115589	26.3551951			44.2043222	124.019608	
	LVIAd	cm^2	126.4	123.3	136.2	133.5	121.2	142.8	103.6	126.714286	12.7227393			103.6	142.8	
	LVIAs	cm^2	53.8	56.3	63	50.1	55.2	56.5	43.1	54	6.16495472			43.1	63	
	SV	mL	756	642	732	766	576	822	518	687.428571	111.173824			518	822	
	SV/kg	mL/kg	1.74595843	1.17367459	1.23648649	1.2557377	1.18032787	1.46263345	1.19354839							
	SV MOD	mL	675	574	668	723	552	765	450	629.571429	109.515383			450	765	
	CO	L/min	26.82	34.37	26.7	29.6	19.02	43.16	17.34	28.1442857	8.85226121			17.34	43.16	
	CO/kg	L/min/kg	0.06193995	0.06283364	0.04510135	0.04852459	0.03897541	0.07679715	0.03995392							
	co mod	L/min	23.97	30.7	24.3	27.95	18.2	40.18	15.08	25.7685714	8.30348607			15.08	40.18	
	rr	ms	1689	1135	1539	1539	1863	1500	1768	1576.14286	236.289673			1135	1863	
	LADLmax	cm	10.6	10.6	12.1	11.6	12.5	12.4	11.4	11.6	0.78951462			10.6	12.5	
Mmode	IVSd	cm	2.6	2.9	2.6	3	2.8	2.9	2.4	2.74285714	0.2149197			2.4	3	
	LVIDd	cm	11	10.6	10.2	11.4	10.7	10.7	9.5	10.5857143	0.60395522			9.5	11.4	
	LVFWd	cm	1.8	2	2	1.9	2.3	2.2	2.1	2.04285714	0.17182494			1.8	2.3	
	IVSs	cm	4.5	4.5	4.4	4.6	4.4	4.2	3.9	4.35714286	0.2370453			3.9	4.6	
	LVIDs	cm	6.2	5.8	5.7	6.5	5.6	6.7	6	6.07142857	0.41518785			5.6	6.7	
	LVFWs	cm	2.9	3.9	3.4	3.8	4	3.5	3.4	3.55714286	0.37796447			2.9	4	
	FS	%	44	45	44	43	48	37	37	42.5714286	4.11732692			37	48	
	RWT		0.4	0.47	0.453	0.431	0.48	0.477	0.48	0.45585714	0.03043807			0.4	0.48	
	MWT	cm	2.2	2.45	2.3	2.45	2.55	2.55	2.25	2.39285714	0.14267846			2.2	2.55	
	LVMass	g	2453.75456	2668.214	2296.65568	3008.83288	2863.44148	2863.44148	1982.785	2591.01787	366.150108			1982.785	3008.83288	
	EPSS	cm	0.3	0.6	0.7	0.2	0.3	0.3	0.5							
	EPSS	mm	3	6	7	2	3	3	5	4.14285714	1.86445447			2	7	
	PEP	ms	65	42	101	66	55	62	83	67.7142857	19.1808436			42	101	
	ET	ms	501	468	416	451	492		476	467.333333	30.7224131			416	501	
	RVIDD	cm	3.1	2.8	2.8	3.1	3.3	3.3	3.2	3.08571429	0.21157009			2.8	3.3	
RVIDS	cm	2.1	2.1	4.2	2.6	3.1	2.8	2.6	2.78571429	0.71978833			2.1	4.2		
TDI	S1	m/s	0.06	0.08	0.07	0.05	0.09	0.07	0.06							
	S1	cm/s	6	8	7	5	9	7	6	6.85714286	1.34518542			5	9	
	SM	m/s	0.08	0.06	0.11	0.11	0.14	0.14	0.13	0.11	0.0305505					
	Sm	cm/s	8	6	11	11	14	14	13	11	0.305505046			6	14	
	E1	m/s	0.075	0.09	0.08	0.07	0.08	0.08	0.08							
	E1	cm/s	7.5	9	8	7	8	8	8	7.92857143	0.6074929			7	9	
	EM	m/s	0.22	0.21	0.21	0.23	0.25	0.27	0.21							
	Em	cm/s	22	21	21	23	25	27	21	22.8571429	2.34012617			21	27	
	AM	m/s	0.09	0.09	0.14	0.11	0.11	0.11	0.07							
	Am	cm/s	9	9	14	11	11	11	7	10.2857143	2.21466971			7	14	
	Em/Am		2.44444444	2.33333333	1.5	2.09090909	2.27272727	2.45454545	3	2.2994228	0.45098412			1.5	3	
	IVCTM	ms	85	104	107	142	118	111	161	118.285714	25.4277688			85	161	
	PEPM	ms	79.5	90	101	97	97	91	94	92.7857143	6.97529655			79.5	101	
	ETM	ms	462	392	447	437	406	471	432	435.285714	28.4939425			392	471	
	IVRTM	ms	65.5	42	42	69	87	62	83	64.3571429	17.740524			42	87	
IMPm	calculated as	0.32575758	0.37244898	0.33333333	0.48283753	0.50492611	0.36730361	0.56481481								
LA Veloc	m/s	0.08	0.09	0.07	0.09	0.08	0.11	0.07								
LA veloc	cm/s	8	9	7	9	8	11	7	8.42857143	1.39727626			7	11		
Global circur%		-17.3	-16.5	-13.6	-12.9	-17.5	-16.8	-16.4					-16.5	-17.05	-17.5	-12.9

Table 8. Raw blood pressure measurements for horses in study.

Measurement #		Horse			
		1	2	3	4
1	Systolic pressure (mm Hg)	112	135	112	134
	Diastolic pressure (mm Hg)	50	84	71	75
	Mean arterial pressure (mm Hg)	71	97	85	97
2	Systolic pressure (mm Hg)	112	129	104	131
	Diastolic pressure (mm Hg)	48	86	65	79
	Mean arterial pressure (mm Hg)	69	98	81	97
3	Systolic pressure (mm Hg)	107	137	111	123
	Diastolic pressure (mm Hg)	44	90	66	78
	Mean arterial pressure (mm Hg)	67	108	85	94

Table 9. Raw correlation data

	SI		SI		Gb		Sg		GEZI		AIRG		DI		Homa-beta		Homa-IR		Ib	
	r	p	rho	p	r	p	r	p	r	p	r	p	rho	p	rho	p	rho	p	rho	p
PAD	0.049527	0.937			-0.49553	0.2581	0.068931	0.8833	-0.49012	0.2642	-0.86739	0.0114	0.6667	0.1019	-0.5586	0.1925	-0.5586	0.1925	-0.6487	0.115
AoD	0.921477	0.0261			-0.34485	0.4487	0.787414	0.0356	0.253032	0.5841	-0.77125	0.0423	0.75	0.0522	-0.8214	0.0234	-0.8929	0.0068	-0.8929	0.0068
LADmax	0.555072	0.3314			0.022017	0.9626	0.206463	0.6569	0.262008	0.5703	0.037346	0.9366	0.2143	0.6445	0	1	-0.1429	0.7599	-0.1429	0.7599
LADmax	-0.0835	0.8938			-0.09659	0.8368	-0.2766	0.5482	-0.54921	0.2016	-0.29354	0.5229	0.1429	0.7599	0.0714	0.879	0.0357	0.9394	0.0357	0.9394
LAAa	0.68605	0.2009	0.9747	0.0048	-0.1534	0.7426	0.619845	0.1376	0.230005	0.6198	-0.71831	0.069	0.4324	0.3325	-0.4865	0.2682	-0.5766	0.1754	-0.5766	0.1754
LAAmin	0.712601	0.1768			-0.27272	0.554	0.514417	0.2375	-0.00367	0.9938	-0.3928	0.3834	0.8571	0.0137	-0.6429	0.1194	-0.7857	0.0362	-0.7857	0.0362
Ac LA FAC	-0.14438	0.8168			0.167086	0.7203	-0.04565	0.9226	0.18331	0.694	-0.14203	0.7613	-0.5714	0.1802	0.2143	0.6445	0.3214	0.4821	0.3214	0.4821
Pa LA FAC	-0.4471	0.4503			-0.0421	0.9286	-0.62025	0.1373	-0.71316	0.072	0.051633	0.9125	0.0357	0.9394	0.2857	0.5345	0.2857	0.5345	0.2857	0.5345
A R-I	-0.35866	0.5533			0.072843	0.8767	-0.47233	0.2845	-0.37691	0.4046	-0.03321	0.9437	0	1	0.2143	0.6445	0.2143	0.6445	0.2143	0.6445
LVIAd	0.545198	0.3419			0.074039	0.8747	0.317282	0.4881	0.302437	0.5097	-0.19063	0.6822	-0.1071	0.8192	0	1	-0.0357	0.9394	-0.0357	0.9394
LVIAs	0.899895	0.0374	0.9	0.0374	-0.2496	0.5893	0.803948	0.0293	0.469574	0.2877	-0.64512	0.1177	0.3929	0.3833	-0.7143	0.0713	-0.6429	0.1194	-0.6429	0.1194
SV	0.37659	0.5321			0.243872	0.5982	0.141993	0.7614	0.28226	0.5397	0.005216	0.9911	-0.2143	0.6445	0.2857	0.5345	0.1786	0.7017	0.1786	0.7017
SV MOD	0.357955	0.5542			0.165491	0.7229	0.098166	0.8342	0.2288	0.6217	-0.00589	0.99	-0.2143	0.6445	0.2857	0.5345	0.1786	0.7017	0.1786	0.7017
CO	0.118553	0.8494			0.30384	0.5077	0.067921	0.885	-0.06454	0.8907	-0.23666	0.6094	0	1	0.1071	0.8192	0.0714	0.879	0.0714	0.879
co mod	0.1161	0.8519			0.271004	0.5566	0.041857	0.929	-0.07433	0.8742	-0.22589	0.6262	0.0714	0.879	0	1	0	1	0	1
rr	-0.51709	0.3723			-0.52825	0.2229	-0.30234	0.5099	0.212715	0.647	-0.24073	0.603	-0.018	0.9694	-0.0541	0.9084	-0.0721	0.878	-0.0721	0.878
LADLmax	0.357818	0.5543			-0.3569	0.432	0.080102	0.8645	0.293892	0.5223	-0.01656	0.9719	0.2342	0.6132	-0.4685	0.289	-0.3424	0.4523	-0.3424	0.4523
LVIDs	-0.54187	0.3455			0.424387	0.3426	-0.53314	0.2179	-0.1247	0.7899	0.436479	0.3275	-0.7143	0.0713	0.75	0.0522	0.75	0.0522	0.75	0.0522
LVIDd	0.02753	0.965			-0.10696	0.8195	-0.25353	0.5833	-0.35232	0.4383	-0.11425	0.8073	0.1261	0.7876	0.3063	0.504	0.036	0.9389	0.036	0.9389
IVSs	0.419142	0.4824			-0.0844	0.8572	0.18292	0.6946	-0.18253	0.6953	-0.27731	0.5471	0.4546	0.3054	0.2	0.6672	-0.1455	0.7556	-0.1455	0.7556
IVSd	0.000462	0.9994			0.022431	0.9619	-0.21596	0.6419	-0.5347	0.2163	-0.20516	0.659	0.3273	0.4736	0.1091	0.8159	0	1	0	1
FS	0.606352	0.2783			-0.53625	0.2147	0.308722	0.5005	-0.15797	0.7352	-0.52823	0.2229	0.9274	0.0026	-0.7092	0.0743	-0.8729	0.0103	-0.8729	0.0103
LVFVWs	-0.06044	0.9231			-0.1422	0.761	-0.13837	0.7673	-0.5863	0.1665	-0.18472	0.6917	0.6847	0.0897	-0.3964	0.3786	-0.3784	0.4026	-0.3784	0.4026
LVFVWd	-0.13675	0.8264			-0.52185	0.2296	-0.09665	0.8637	-0.12592	0.7879	-0.31945	0.4849	0.1261	0.7876	-0.5225	0.2289	-0.2342	0.6132	-0.2342	0.6132
RWT	-0.13386	0.8301			-0.14373	0.7585	0.003162	0.9946	-0.16897	0.7172	-0.19477	0.6756	0	1	-0.3424	0.4523	-0.036	0.9389	-0.036	0.9389
MWT	-0.07378	0.9062			-0.29733	0.5172	-0.22085	0.6342	-0.47853	0.2773	-0.34687	0.4459	0.4183	0.3504	-0.4183	0.3504	-0.3091	0.4999	-0.3091	0.4999
LVMass	-0.04258	0.9458			-0.22155	0.6331	-0.31222	0.4954	-0.50787	0.2446	-0.23713	0.6087	0.3424	0.4523	0.0541	0.9084	-0.0721	0.878	-0.0721	0.878
EPSS	0.635082	0.2496			0.255978	0.5795	0.797235	0.0318	0.461087	0.2977	-0.20507	0.6591	0.1482	0.7511	-0.4818	0.2736	-0.3336	0.4647	-0.3336	0.4647
PEP	0.655831	0.2295			0.298585	0.5154	0.471678	0.2853	0.871448	0.0106	0.498009	0.2554	-0.4643	0.2939	0.3571	0.4316	0.3571	0.4316	0.3571	0.4316
ET	-0.74895	0.251			-0.55614	0.2518	-0.64392	0.1676	-0.55363	0.2544	-0.28404	0.5854	-0.1429	0.7872	-0.0857	0.8717	0.0286	0.9572	0.0286	0.9572
RVIDd	-0.87196	0.0539			-0.44091	0.3221	-0.73364	0.0606	-0.26135	0.5713	0.144456	0.7573	-0.2753	0.5501	0	1	0.1652	0.7234	0.1652	0.7234
RVIDs	0.85713	0.0624			-0.10147	0.8286	0.678828	0.0936	0.754632	0.0499	0.009802	0.9834	0.2182	0.6383	-0.5274	0.2238	-0.4001	0.3738	-0.4001	0.3738
S1	0.526882	0.3616			-0.71854	0.0689	0.324853	0.4771	-0.14189	0.7615	-0.86115	0.0128	0.6728	0.0976	-0.9274	0.0026	-0.8001	0.0307	-0.8001	0.0307
Sm	-0.24596	0.69			-0.29271	0.5241	-0.26687	0.5629	0.186669	0.6886	0.252292	0.5852	-0.1818	0.6964	-0.1818	0.6964	0.0364	0.9383	0.0364	0.9383
PEPm	0.418407	0.4832			0.109025	0.816	0.288961	0.5297	0.221435	0.6332	0.253494	0.5833	0.3063	0.504	-0.2523	0.5852	-0.2342	0.6132	-0.2342	0.6132
IVCTm	-0.51672	0.3727	-0.9	0.0374	0.381262	0.3987	-0.49074	0.2635	-0.22361	0.6298	0.757769	0.0484	-0.2857	0.5345	0.3571	0.4316	0.5	0.2532	0.5	0.2532
ETm	0.153744	0.805			0.184498	0.6921	-0.00328	0.9944	0.589989	0.1632	0.314471	0.4921	-0.5714	0.1802	0.25	0.5887	0.25	0.5887	0.25	0.5887
E1	0.216177	0.7279			-0.10118	0.8291	0.394836	0.3807	-0.15004	0.7481	-0.64911	0.1147	0.2955	0.5199	-0.6108	0.1451	-0.3744	0.4081	-0.3744	0.4081
Em	-0.22114	0.7207			-0.44188	0.3209	-0.37355	0.4091	-0.17576	0.7062	-0.23201	0.6166	0	1	-0.0371	0.9371	-0.0371	0.9371	-0.0371	0.9371
Em/Am	-0.92112	0.0263			-0.01255	0.9787	-0.73507	0.0598	-0.50075	0.2523	0.17998	0.6994	-0.7143	0.0713	0.3571	0.4316	0.5714	0.1802	0.5714	0.1802
IVRTm	-0.9976	0.0072	-0.9	0.0374	-0.43444	0.33	-0.73655	0.059	-0.32934	0.4707	0.295215	0.5204	-0.0901	0.8477	0.1982	0.6701	0.1982	0.6701	0.1982	0.6701
Am	0.892035	0.0419			-0.10993	0.8145	0.638602	0.1227	0.560311	0.1908	-0.17715	0.704	0.4304	0.3351	-0.4491	0.3121	-0.5052	0.2474	-0.5052	0.2474
LA veloc	-0.25789	0.6753			0.070728	0.8802	-0.34623	0.4468	-0.39171	0.3848	-0.20096	0.6657	0.0367	0.9377	0.1468	0.7534	0.1285	0.7837	0.1285	0.7837
SP	-0.61191	0.5808			0.787821	0.2122	-0.74639	0.2536	-0.5783	0.4217	0.809997	0.19	0	1	0.8	0.2	0.8	0.2	0.8	0.2
DP	0.112246	0.9284			0.799183	0.2008	-0.03098	0.969	-0.51898	0.481	0.007179	0.9928	0.8	0.2	0	1	0	1	0	1
MAP	-0.02636	0.9832			0.837259	0.1627	-0.14107	0.8589	-0.58405	0.416	0.093498	0.9065	0.8	0.2	0	1	0	1	0	1
age	-0.04739	0.9397			-0.78318	0.0373	0.02615	0.9556	0.152364	0.7443	-0.40227	0.371	0.0727	0.8768	-0.3819	0.3979	-0.3819	0.3979	-0.3819	0.3979
weight	0.522978	0.3659			0.415815	0.3535	0.3323124	0.4796	0.101102	0.8292	0.095782	0.8381	0.2143	0.6445	0.0357	0.9394	0	1	0	1
IMPM	-0.67554	0.2107																		
	rho	p			rho	p	rho	p	rho	p	rho	p								
GSC	-0.2	0.7471			0.892															

VITA

Natasha Jane Williams

Candidate for the Degree of

Master of Science

Thesis: INVESTIGATING THE RELATIONSHIP BETWEEN CARDIAC FUNCTION
AND INSULIN SENSITIVITY IN HORSES

Major Field: Veterinary Biomedical Sciences

Biographical:

Education:

Completed the requirements for the Master of Science in Veterinary Biomedical Sciences at Oklahoma State University, Stillwater, Oklahoma in December, 2021.

Completed the requirements for the Bachelor of Veterinary Science at University of Melbourne, Melbourne, Victoria, Australia in 2013.

Completed the requirements for the Bachelor of Science in Molecular and Drug Design at University of Adelaide, Adelaide, South Australia, Australia in 2008.

Experience:

Private mixed practice, rotating equine internship, residency in large animal internal medicine (food animal emphasis).

Professional Memberships:

ANZCVS (Equine Medicine)